Partial decay widths and form factor implementation for the simulation of the Λ_c^+ decays in SHERPA

vorgelegt von

Sven Schiffner
geboren am 28.10.1994 in Sebnitz

Institut für Kern- und Teilchendphysik
Fachrichtung Physik
Fakultät Mathematik und Naturwissenschaften
Technische Universität Dresden
2017

Eingereicht am 24. Mai 2017

1. Gutachter: Dr. Frank Siegert
2. Gutachter: Prof. Dr. Michael Kobel

Summary

Abstract
English:

Abstract
Deutsch

Contents

A Appendix   **39**

1 Introduction

One of the big questions of mankind is, why are we here. And the correspondending question in physics is, why more matter than anti-matter exists in the universe. This thesis cannot clear the question but it can be a part of the big picture.

The `LHC` (Large Hadron Collider) is one of the biggest experiments of humanity. This accelerator collides proton with protons, lead nuclei with protons or lead nuclei with lead nuclei. One detector of this big apparatus is the `LHCb`. The `LHCb` is a try to find the answer of the above question. It examines asymmetries in the decay of matter and anti-matter mainly for proton-proton-collissions. And so deviations from the Standard Model. The Standard Model is a theory that describes the fundamental interactions between and the elementary particles itself very well. These deviations can result in additions to the Standard Model to consider a asymmetry between matter and anti-matter, and so lead to an answer for the matter surplus. For this the results from the experiment have to be compared to the theoratical results. But simulations are needed for the theoretical results. This comes from the different interactions that happens through a particle collision. A lot of particles are created and decay. On of the simulation tools is `Sherpa`[7]. This program use Monte-Carlo techniques to obtain results.

One possible baryon that can be created is the Λ_c^+. It is the lightest baryon that contains a charm quark. The charm quark is like the up quark, that builds neutrons and protons together with the down quark, but heavier.

For a good comparison between the experimental results and the theoretical simulations it is important to implement brayons and not only bare quarks in the simulation. The behavior of quarks in bound states is different to free quarks that didn't exists in nature. So the hadronization and the the decay of the hadrons are important processes. This processes have to be recognized to get good theoratical predictions..

This thesis has the goal to improve the simulation through a better implementation of the Λ_c^+ decays.

I want to thanks Johannes Krause, Daniel Reichelt and Sebastian Liebschner for their help.

2 Basic Physical Principles

2.1 Baryons

A baryon is a subatomic particle. It is composite and contains three quarks. The baryons form together with the mesons the class of the hadrons. Mesons are composed of two quarks, one quark and one antiquark.

Protons and neutrons which are the components of our normal matter are baryons. These are the lightest baryons. The proton is made of two up quarks and one down quark. The neutron contains two down quarks and one up quark.

All observed events so far feature that the number of baryons in a reaction is observed. To use this in calculations every quark get the baryon number $B = 1/3$ and every anti-quark $B = -1/3$. In a decay from a baryon ($\sum B = 1$) the final products has to be a baryon ($\sum B = 1$) or two baryons ($\sum B = 2$) and an anti-baryon ($\sum B = -1$) and so on.

2.1.1 Λ_c^+ Baryon

The Λ_c^+ has a mass of $2286.46 \pm 0.14 \text{MeV}$[4] and a mean life time of $(2.00 \pm 0.06) \cdot 10^{-13} \text{s}$[4]. It is one of the lightest charmed baryons and is made of one up, down and charm quark. Its charge is $+1$ of the electron charge[4].

2.2 Decays

Decays are processes with one particale in the initial state and n particles in the final state for n= 2,3,.... The decayed particle must not be in the final state. This makes the difference to radiation processes. The decay process can always be transformed in to the rest mass frame of the Decayer and so the summation over the energy of all particles in the final state has to be the rest energy of the decaying particle.

A decay process or more general a transision process is characterized through Fermi's golden rule:

$$\Gamma_{fi} = 2\pi |T_{fi}|^2 \rho\left(E_i\right), \tag{2.1}$$

where T_{fi} is the transition matrix element and $\rho(E_i)$ is the density of states. The result is the transition rate Γ_{fi}. In natural units the unit of the transition rate is GeV^{-1}.

The Γ_{fi} is also called partial decay width. And is characteristic value for a decay process. The sum over all partial decay widths is called total decay width:

$$\Gamma_i = \sum_f \Gamma_{fi}. \tag{2.2}$$

The total width(2.2) is an criterion for the lifetime of the decaying particle. The lifetime of the particle in natural units is the inverse of Γ_i:

$$\tau_i = \frac{1}{\Gamma_i}. \tag{2.3}$$

The branching ratio is the probability to decay in a specific final state. It can be calculated with the partial and total decay width:

$$BR(i \to f) = \frac{\Gamma_f}{\Gamma}. \tag{2.4}$$

2.3 Weak Decay

A weak decay is the transition of a particle through the weak interaction. An elementary particle that is possibly part of an composite can in this way decay to a $\text{W}^{\pm}$-Boson and a correspondending particle. But the W-Boson only couple to lef-handed fundamental partciles and right-handed fundamental anti-particles. The spinor for the weak interaction than looks like (2.5). There the upper particle have isospin -1/2 and the lower isospin +1/2.

$$\begin{pmatrix} \nu_e \\ e^- \end{pmatrix}_L, \begin{pmatrix} \nu_\mu \\ \mu^- \end{pmatrix}_L, \begin{pmatrix} s \\ c \end{pmatrix}_L, \begin{pmatrix} e^+ \\ \bar{\nu}_e \end{pmatrix}_R, \begin{pmatrix} \mu^+ \\ \bar{\nu}_\mu \end{pmatrix}_R \quad \text{etc.} \tag{2.5}$$

In (2.5) only the particles are shown that are relevant for this thesis.

In the Feynman diagram 2.1 the semileptonic decay of a Λ_c^+ is visible. The up and down quark from the Λ_c^+ are unchanged. They can only influence the transition matrix element through a different behavior of the charm quark. The charm quark transforms through the weak decay in to a down or strange quark. The down quark forms with the other two qarks a neutron and the strange quark a Λ.The emitted W^+-Boson decays leptonic in an anti-lepton and the correspondending neutrino. Other decays of the W^+-boson are possible. For this thesis only the semileptonic decays channels are relevant. The complete dynamic of the process will be discussed in 2.4. In this section we will take a closer look at the $\text{W}^{\pm}$ propagator.

The value for a $\text{W}^{\pm}$ propagator is $\frac{g_w^2}{8}\frac{1}{q^2-m_W^2}$. The transferred momentum is $q^2 = (p_f - p_i)^2$. It is limited by the initial state mass and for most decays this is much less than the mass of the
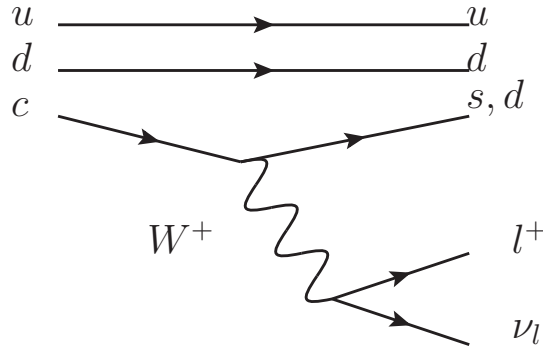
Figure 2.1: Semileptonic decay modes of the Λ_c^+ into a neutron (udd) or a Λ (uds), an positron or an anti-muon and the correspondending neutrino (own graphic)

$W^\pm$ boson. The last fraction can be approximated through $-\frac{1}{m_W^2}$. The whole term becomes to $-\frac{g_w^2}{8m_W^2}$ and this is the Fermi coupling constant G_F except a factor $-\frac{1}{sqrt2}$:

$$\frac{G_F}{\sqrt{2}} = \frac{g_w^2}{8m_W^2}$$

The weak decay has in this approximation a threesome vertex with the coupling constant G_F.

2.4 V-A current

The value of a vertex where two matching leptons transforms into a $W^\pm$ boson is $-i\frac{g}{2\sqrt{2}}\gamma^\mu\left(1-\gamma^5\right)$. If the sum is splitted, the the term without γ^5 is called vector and the part with the γ^5 axial-vector through the geometrical effect of the γ-matrix. The transition from quarks needs an additional factor V_{if}. i is the quark and in the initial state and f the quark in the final state. The factor comes from the CKM-matrix[2]. The matrix from [2] is

$$V_{CKM} = \begin{bmatrix} 0.97434^{+0.00011}_{-0.00012} & 0.22506 \pm 0.00050 & 0.00357 \pm 0.00015 \\ 0.22492 \pm 0.00050 & 0.97351 \pm 0.00013 & 0.0411 \pm 0.0013 \\ 0.00875^{+0.00032}_{-0.00033} & 0.0403 \pm 0.0013 & 0.99915 \pm 0.00005 \end{bmatrix}. \tag{2.6}$$

With the general Feynman rules for vertices and propagators the transition matrix element becomes to (2.7) like in [13, Eq. 1].

$$T = \frac{G_F}{\sqrt{2}} V_{Qq} \bar{u}_l \gamma^\mu \left(1-\gamma^5\right) u_{\nu_l} \langle B(p',s')|J_\mu|\Lambda_c(p,s)\rangle \tag{2.7}$$

The B in (2.7) stands for the neutron or Λ. The current J_μ can be splitted in a vector and an axial-vector part $J_\mu = V_\mu - A_\mu$ like in (2.8).

$$\langle B(p', s')|V_\mu|\Lambda_c(p, s)\rangle = \bar{u}(p', s') \left(F_1(q^2)\gamma_\mu + F_2(q^2)\frac{p_\mu}{m_{\Lambda_c}} + F_3(q^2)\frac{p'_\mu}{m_B} \right) u(p, s)$$

$$\langle B(p', s')|A_\mu|\Lambda_c(p, s)\rangle = \bar{u}(p', s') \left(G_1(q^2)\gamma_\mu + G_2(q^2)\frac{p_\mu}{m_{\Lambda_c}} + G_3(q^2)\frac{p'_\mu}{m_B} \right) \gamma^5 u(p, s) \quad (2.8)$$

The F_i and G_i are form factors for the transition. They are specific for the initial and final baryons and describe the different behavior of the quarks in a bound state in contrast to the free decay. The functional behavior of these form factors is related to $q^2 = (p - p')^2$.

2.5 Monte-Carlo methods

The `Sherpa` software use Monte-Carlo methods to calculate the decay widths and randomly select the dynamics of a process. In my thesis I did not work on the Monte-Carlo algorithms. For details about these methods the diploma[15] from Dr. Frank Siegert can be considered.

3 Methods and Implementation

3.1 Decay table

`Sherpa` uses for the decays from all kinds of particles the decay channels and branching ratios from a decay table. This table has to be updated manually with data from the Particle Data Group (PDG) because there exists no analytic calculations for the first principles. Also data from other sources are included, e.g. EvtGen. But a big amount of decay channel and branching ratios is taken from the PDG.

Newer measurements of particle decays are more accurate and so it is important to keep the decay table up to date. This will reduce the uncertainties for the branching ratios and so all kinds of results that are taken from a simulation.

A lot of changes were needed to update the decay table. An little abstract of the changes are visible below:

Table 3.1: Extract of the changes in the Decays.dat from the Λ_c^+

Decay	BR(Delta BR)[Origin]	
	old	new
Modes with nucleons/Deltas		
$\Lambda_c^+ \to P^+ + K_b$	0.023(0.006)[PDG]	-
$\Lambda_c^+ \to P^+ + K_s$	-	0.0158(0.0008)[PDG]
$\Lambda_c^+ \to P^+ + K^- + \pi^+$	0.028(0.008)[PDG]	0.035(0.004)[PDG]
$\Lambda_c^+ \to P^+ + K_b + \pi$	0.033(0.010)[PDG]	0.0199(0.0013)[PDG]
$\Lambda_c^+ \to P^+ + \pi^+ + \pi^+ + \pi^- + \pi^-$	0.018(0.012)[PDG]	0.0023(0.0015)[PDG]
S = 0		
$\Lambda_c^+ \to P^+ + f(0980)$	0.0028(0.0019)[PDG]	0.0035(0.0023)[PDG]
S = 0		
$\Lambda_c^+ \to P^+ + \pi^+ + \pi^-$	0.0007(0.0007)[PDG]	-
S = 0		
$\Lambda_c^+ \to \Delta(1232)^{++} + K^-$	0.0086(0.003[PDG]	0.0109(0.0025)[PDG]
Modes with hyperons		
$\Lambda_c^+ \to \Lambda + \pi^+$	0.0107(0.0028)[PDG]	0.0130(0.0007)[PDG]
$\Lambda_c^+ \to \Lambda + \pi^+ + \pi$	-	0.071(0.0004)[PDG]

$\Lambda_c^+ \to \Lambda + \rho(770)^+$	-	0.036(0.013)[PDG]
S = 0		
$\Lambda_c^+ \to \Lambda + K^+$	0.0005(0.00016)[PDG]	0.00061(0.00012)[PDG]
$\Lambda_c^+ \to \Sigma^- + \pi^+ + \pi^+$	-	0.021(0.004)[PDG]
semileptonic modes		
$\Lambda_c^+ \to \Lambda + \nu_e + e^+$	0.021(0.006)[PDG]	0.036(0.004)[PDG]
$\Lambda_c^+ \to \Lambda + \nu_\mu + \mu^+$	0.020(0.007)[PDG]	0.036(0.004)[PDG]

The table above shows that the decay channel

$$\Lambda_c^+ \to P^+ + K_b$$

was replaced by

$$\Lambda_c^+ \to P^+ + K_s.$$

The decay

$$\Lambda_c^+ \to P^+ + \pi^+ + \pi^-$$

was removed because the process is included in

$$\Lambda_c^+ \to P^+ + f(0980)$$

due to the decay of the f(0980):

$$f(0980) \to \pi^+ + \pi^-.$$

The full list of changes can be found at A.1.
The semileptonic decay of the Λ_c^+ into a neutron is important for further considerations.

Table 3.2: Decays in a neutron in the Decays.dat from the Λ_c^+

Decay	BR(Delta BR)[Origin]
semileptonic modes	
$\Lambda_c^+ \to n + \nu_e + e^+$	0.003[EvtGen]
$\Lambda_c^+ \to n + \nu_\mu + \mu^+$	0.003[EvtGen]

The branching for these semileptonic decays are not taken from the PDG because no actual experimental data exists. The reason is that most of the modern detectors can't detect neutrons

very well. This comes from the neutral electric charge and the long lifetime of the neutron. An improved measurement would be recommended because this processes are important for the form factor calculation. The neutron is often considered as the final decay state of the Λ_c^+. All these changes leads to a sum of all branching ratios from $87, 98\%$. This is near to 100%. But there are still missing some branching ratios.

3.2 Another Form Factor parametrization

The two formulas in (2.8) show one popular parametrization for the V-A-Current another possible and popular writing is given in (3.1).

$$\langle B(p',s')|V_\mu|\Lambda_c(p,s)\rangle = \bar{u}(p',s')\left(f_1^V(q^2)\gamma_\mu + f_2^V(q^2)i\sigma_{\mu\nu}\frac{q^\nu}{m_{\Lambda_c}} + f_3^V(q^2)\frac{q_\mu}{m_{\Lambda_c}}\right)u(p,s)$$

$$\langle B(p',s')|A_\mu|\Lambda_c(p,s)\rangle = \bar{u}(p',s')\left(f_1^A(q^2)\gamma_\mu + f_2^A(q^2)\sigma_{\mu\nu}\frac{q^\nu}{m_{\Lambda_c}} + f_3^A(q^2)\frac{q_\mu}{m_{\Lambda_c}}\right)\gamma^5 u(p,s)$$

$$(3.1)$$

In this notation is $q = p-p'$. A convsersion formula is now needed for the different parametrizations of the current. The equations in [5, Eq. 15] give one direction for transformation. But most of the following form factors are in the form with p and p' and not with q. So the inversion of the given transformation would be the easiest way to get a decent formula. The first step is to create a transformation matrix like below out of the formulas in [5, Eq. 15].

$$\begin{pmatrix} f_1^V \\ f_2^V \\ f_3^V \\ f_1^A \\ f_2^A \\ f_3^A \end{pmatrix} = \begin{bmatrix} 1 & \frac{m_{\Lambda_c}+m_B}{2m_{\Lambda_c}} & \frac{m_{\Lambda_c}+m_B}{2m_B} & 0 & 0 & 0 \\ 0 & -\frac{1}{2} & -\frac{m_{\Lambda_c}}{2m_B} & 0 & 0 & 0 \\ 0 & \frac{1}{2} & -\frac{m_{\Lambda_c}}{2m_B} & 0 & 0 & 0 \\ 0 & 0 & 0 & 1 & -\frac{m_{\Lambda_c}-m_B}{2m_{\Lambda_c}} & -\frac{m_{\Lambda_c}-m_B}{2m_B} \\ 0 & 0 & 0 & 0 & -\frac{1}{2} & -\frac{m_{\Lambda_c}}{2m_B} \\ 0 & 0 & 0 & 0 & \frac{1}{2} & -\frac{m_{\Lambda_c}}{2m_B} \end{bmatrix} \cdot \begin{pmatrix} F_1 \\ F_2 \\ F_3 \\ G_1 \\ G_2 \\ G_3 \end{pmatrix} \quad (3.2)$$

The block structure of the matrix is a mathemtaical manifestation of the independence of the vector and axial-vector part. This matrix can be splitted in two equations:.

$$\begin{pmatrix} f_1^V \\ f_2^V \\ f_3^V \end{pmatrix} = \begin{bmatrix} 1 & \frac{m_{\Lambda_c}+m_B}{2m_{\Lambda_c}} & \frac{m_{\Lambda_c}+m_B}{2m_B} \\ 0 & -\frac{1}{2} & -\frac{m_{\Lambda_c}}{2m_B} \\ 0 & \frac{1}{2} & -\frac{m_{\Lambda_c}}{2m_B} \end{bmatrix} \cdot \begin{pmatrix} F_1 \\ F_2 \\ F_3 \end{pmatrix} \text{ and}$$

$$\begin{pmatrix} f_1^A \\ f_2^A \\ f_3^A \end{pmatrix} = \begin{bmatrix} 1 & -\frac{m_{\Lambda_c}-m_B}{2m_{\Lambda_c}} & -\frac{m_{\Lambda_c}-m_B}{2m_B} \\ 0 & -\frac{1}{2} & -\frac{m_{\Lambda_c}}{2m_B} \\ 0 & \frac{1}{2} & -\frac{m_{\Lambda_c}}{2m_B} \end{bmatrix} \cdot \begin{pmatrix} G_1 \\ G_2 \\ G_3 \end{pmatrix} . \quad (3.3)$$

The matrices can be inverted if the determinant is unequal to zero. The determinant of both matrices are the same. This comes from the block structure with the zeroes in the first column. The value for the determinant is

$$det(\dots) = \frac{m_{\Lambda_c}}{2m_B}. \tag{3.4}$$

If the mass of the Λ_c^+ is nonzero than the matrices are invertible, which is obviously true. The matrix for G_i is similar to the matrix for F_i. So it is enough to invert one matrix and compare with the other. The resulting matrices are:

$$\begin{pmatrix} F_1 \\ F_2 \\ F_3 \end{pmatrix} = \begin{bmatrix} 1 & \frac{3m_{\Lambda_c}+m_B}{4m_{\Lambda_c}} & -\frac{m_{\Lambda_c}+m_B}{4m_B} \\ 0 & -1 & 1 \\ 0 & -\frac{m_B}{2m_{\Lambda_c}} & -\frac{m_B}{2m_{\Lambda_c}} \end{bmatrix} \cdot \begin{pmatrix} f_1^V \\ f_2^V \\ f_3^V \end{pmatrix} \quad \text{and}$$

$$\begin{pmatrix} G_1 \\ G_2 \\ G_3 \end{pmatrix} = \begin{bmatrix} 1 & -\frac{3m_{\Lambda_c}-m_B}{4m_{\Lambda_c}} & \frac{m_{\Lambda_c}+m_B}{4m_B} \\ 0 & -1 & 1 \\ 0 & -\frac{m_B}{2m_{\Lambda_c}} & -\frac{m_B}{2m_{\Lambda_c}} \end{bmatrix} \cdot \begin{pmatrix} f_1^A \\ f_2^A \\ f_3^A \end{pmatrix}. \tag{3.5}$$

And finally for every form factor a transformation formula can be obtained:

$$F_1 = f_1^V + \frac{m_{\Lambda_c} + m_B}{4} \left(\frac{3f_2^V}{m_{\Lambda_c}} - \frac{f_3^V}{m_B} \right)$$

$$F_2 = -f_2^V + f_3^A$$

$$F_3 = -\frac{m_B}{2m_{\Lambda_c}} \left(f_2^V + f_3^V \right)$$

$$G_1 = f_1^A + \frac{m_{\Lambda_c} - m_B}{4} \left(-\frac{3f_2^V}{m_{\Lambda_c}} + \frac{f_3^V}{m_B} \right)$$

$$G_2 = -f_2^A + f_3^A$$

$$G_3 = -\frac{m_B}{2m_{\Lambda_c}} \left(f_2^A + f_3^V \right). \tag{3.6}$$

These transformation formulas have been added to `Sherpa`.

3.3 Existing Form Factor implementation in `Sherpa`

First it is important to know wich current parametrization is already used for baryon baryon transitions in `Sherpa`. With this information the right form factor parametrization can be choosen. For a natural transition between two baryons the different coefficient are computed

as:

$$c_{R1} = V_1 - A_1$$
$$c_{L1} = -V_1 - A_1$$
$$c_{R2} = V_2 - A_2$$
$$c_{L2} = -V_2 - A_2$$
$$c_{R3} = V_3 - A_3$$
$$c_{L3} = -V_3 - A_3. \tag{3.7}$$

A natural transition means that the decayer and the daughter baryon have the same parity. V_i and A_i comes from the choosen from factor model for the transition. They are other names for F_i and G_i. The current

$$V_\mu = L_\mu(1, h_1, 0, h_0, c_{R1}, c_{L1})+$$
$$\frac{p_{0,\mu}}{m_0} \cdot Y(1, h_1, 0, h_0, c_{R2}, c_{L2})+$$
$$\frac{p_{1,\mu}}{m_1} \cdot Y(1, h_1, 0, h_0, c_{R3}, c_{L3}) \tag{3.8}$$

is sumed over all possible helicities from the decaying h_0 and the daughter baryon h_1. The definition of L_μ is given in [15, Eq. A.96] and the Y in [15, Eq. A.94]. These are internal functions of `Sherpa`. They are defined as

$$L_\mu(1, h_1, 0, h_0, c_{R1}, c_{L1}) = \bar{u}(p_1, h_1)\gamma_\mu (c_{R1}P_R + c_{L1}P_L) u(p_0, h_0)$$
$$Y(1, h_1, 0, h_0, c_{R2}, c_{L2}) = \bar{u}(p_1, h_1) (c_{R2}P_R + c_{L2}P_L) u(p_0, h_0)$$
$$Y(1, h_1, 0, h_0, c_{R3}, c_{L3}) = \bar{u}(p_1, h_1) (c_{R3}P_R + c_{L3}P_L) u(p_0, h_0). \tag{3.9}$$

The projection operators that are used in (3.9) are defined as

$$P_R = \frac{1}{2} (1 + \gamma_5)$$
$$P_L = \frac{1}{2} (1 - \gamma_5). \tag{3.10}$$

This all equations together form a current wich is similar to $\{(2.8)$. This can also easily been seen through the signs of the γ_5 and the signs of the c_R and c_L. All other current parametrization have to be converted to observe the existing behavior.

3.4 Form Factor Models

3.4.1 Covariant Confined Quark Model (CCQM)

The idea behind the covariant confined quark model ([8], [9]) is to use two loops Feynman diagrams with free quark propagators. This model was developed for mesons but is extended to baryons. It is also possible to successfully calculate tetraquark states with this theory.
For the transition to $\Lambda + l^+ + \nu_l$ [9] was considered and for $n + l^+ + \nu_l$ [8]. The parametrization of the form factor is given by

$$f(q^2) = \frac{F(0)}{1 - as + bs^2} \text{ with } s = \frac{q^2}{m_{\Lambda_c}}. \tag{3.11}$$

The parameters F(0), a and b are taken from the numerical results of [9].

3.4.2 Non relativistic Quark Model (NRQM)

Baryons with a heavy quark possesses a special symmetry. This symmetry is called heavy quark symmetry. The main impact to the characteristics of the baryon results from the degrees of freedom of the light quarks and are independent from the degrees of freedom of the heavy quark. [11]
This form factor model can be used to calculate transistions to excited Λ baryons [11]. The parametrization of the form factors a more complicated compared to the other ones:

$$F = \left(a_0 + a_2 q^2 + a_4 q_4\right) e^{-\frac{3 m_\sigma^2 p_\Lambda^2}{2 m_\Lambda^2 \alpha_{\lambda\lambda'}^2}}$$

$$p_\Lambda = \frac{1}{2m_\Lambda} \lambda^{\frac{1}{2}} (m_{\Lambda_c}^2, m_\Lambda^2, q^2)$$

$$\lambda(x, y, z) = x^2 + y^2 + z^2 - 2xy - 2yz - 2zx \text{ (triangle function)}$$

$$\alpha_{\lambda\lambda'} = \sqrt{\frac{\alpha_\lambda^2 + \alpha_{\lambda'}^2}{2}}, \tag{3.12}$$

where m_σ is the mass of the light quark obtained from [11, p. 13/I] and the α_λ are size parameters of the baryons from [11, p. 13/II].

3.4.3 Light-Cone Sume Rule (LCSR)

The light-cone sum rule is a very famous technique in the class of QCD sum rules[10]. The basic idea is that the vacuum condensates carry no momentum. The light-cone expansion is used with increasing twist. The transition from Λ_c^+ into $\Lambda + l^+ + \nu_l$ is computed with this model in [10].
The parametrization is very simple due to the same values for the first two axial-vector and

vector form factors:

$$f_1^V = f_1^A$$
$$f_2^V = f_2^A$$
$$f_i(q^2) = \frac{f_i(0)}{a_2 s^2 + a_1 s + 1} \text{ with } s = \frac{q^2}{m_{\Lambda_c}}.$$

(3.13)

$f_i(0)$, a_2 and a_1 are parameters of this parametrization. Only the first two form factors are nonzero.

3.4.4 Relativistic Quark Model (RQM)

The relativistic quark model[6] is based on the diquark wave function and the baryon wave function of the bound quark-diquark state. The calculation were done with relativistic quasipotential equation of the Schrödinger type. All computation were relativistically done.

It can predict senmileptonic transitions into n as well as into Λ. The parametrization(3.14) was done until a very high order of the q^2.

$$F(q^2) = \frac{F(0)}{1 - \sigma_1 s + \sigma_2 s^2 + \sigma_3 1 s^3 + \sigma_4 s^4} \text{ with } s = \frac{q^2}{m_{\Lambda_c}}$$

(3.14)

3.4.5 QCD Sum Rule (QCDSR)

Nonperturbative aspects are used in this sum rule [1]. The approach of the QCD sum rule is the expansion in local operators. $\Lambda + l^+ + \nu_l$ is considered in the article.

In this Model two different parametrizations exists. The pole parametrization (3.15) is used like in the other models. But this pole parametrization is a lot simpler due to the relations between the form factors.

$$f_1^A = -f_1^V$$
$$f_2^A = f_2^V$$
$$f_i^V(q^2) = \frac{a_0}{a_1 - q^2}$$

(3.15)

The other form of the parametrization (3.16) is more complicated but interesting due to the exponential ansatz.

$$f_1^A = -f_1^V$$
$$f_2^A = -f_2^V$$
$$f_1^V(q^2) = e^{\frac{q^2 - a_1}{a_0}}$$
$$f_2^V(q^2) = \frac{a_0}{a_1 - q^2} \tag{3.16}$$

The third form factor is zero in both cases.

4 Evaluation and Discussion

4.1 Decay table

The decays of the Λ_c^+ were simulated with the old and the new decay table. 100000000 decay events were used. This leads to a low statistic uncertainty. This section should show the impact of my changes in the decay table. Selected inclusive modes are used to show the difference. The observables multiplicity and energy are used for the comparison. The multiplicity is the number of created particles from the choosen type at the consideres state. The energy is measured by the squared four-momentum of the particles from the choosen type.

The figures in the following section can also be found in the appendixA.2. These figures only show the measurement of the particles after the primary decay of the Λ_c^+. The direct impact due to the changes in the decay table is so better visible. The figures for the measurement at the final state of the decay chain are in A.3.
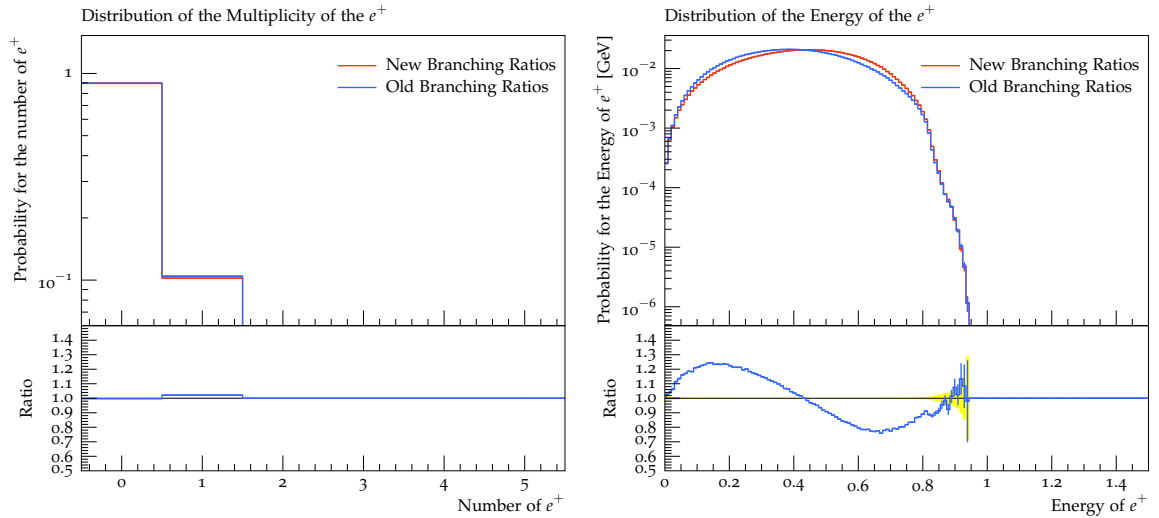
Figure 4.1: multiplicity and energy spectrum of the e^+

In the figures 4.1 and 4.2 you can see that the change of the branching ratios of the semileptonic decays resulting in a nearly equal multiplicity distribution but a significant different energy spectrum for both leptons. The cut-off at the beginning of the muon energy spectrum comes from the bigger rest mass than the electron.This energy is needed to create a detectable on-shell muon.
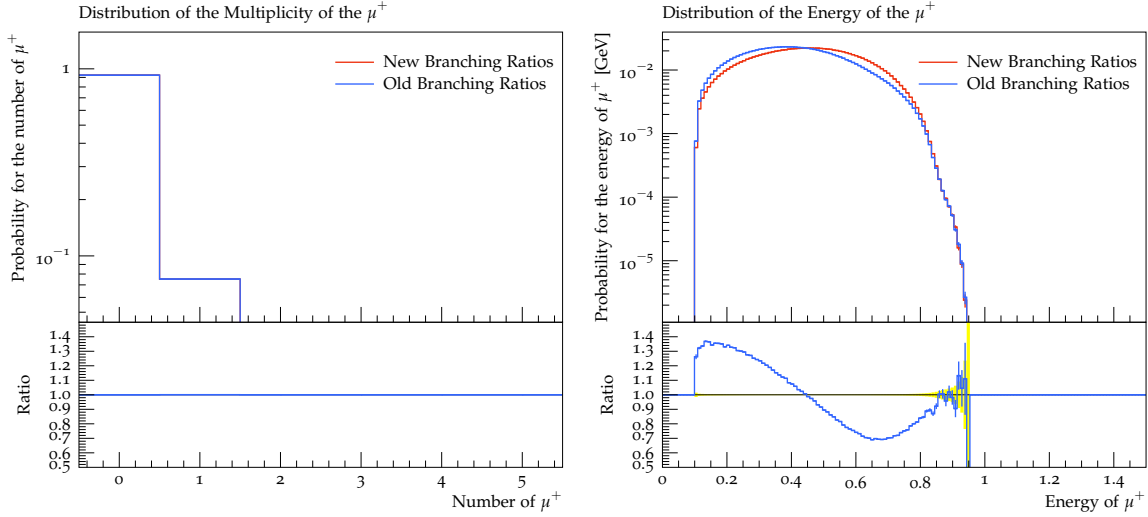
Figure 4.2: multiplicity and energy spectrum of the μ^+

The two main processes to create leptons are the semileptonic decays

$$\Lambda_c^+ \rightarrow \Lambda + l^+ + \nu_l$$

and

$$\Lambda_c^+ \rightarrow n + l^+ + \nu_l.$$

Only the branching ratios for the processes with the Λ in the final state were changed. The higher rest mass of the Λ compared to the neutron leads to leptons with a lower energy. The braching ratios for the neutron decays are the same as before but the branching ratio for the semileptonic Λ decays were increased. T he increase of the branching ratio is visible as the energy shift in the energy spectrum.

The multiplicity didn't changed much because both processes have the same multiplicity. The probability for one positron becomes a little lower. This leads from the lower increase of the branching ratio of the electron compared to the muon.

These changes in the primary decay leads also to changes in the further decays. The figures for the measurement of the particles after the whole decay chain in A.3 look really the same. The plots 4.3 from the π^+ show drastic changes. This changes will be discussed in the following paragraph. Due to the update of the decay table the probability for multiplicity zero and one processes becomes equal. This leads mainly from the processes

$$\Lambda_c^+ \rightarrow \Sigma(1385)^+ + \pi^+ + \pi^-$$
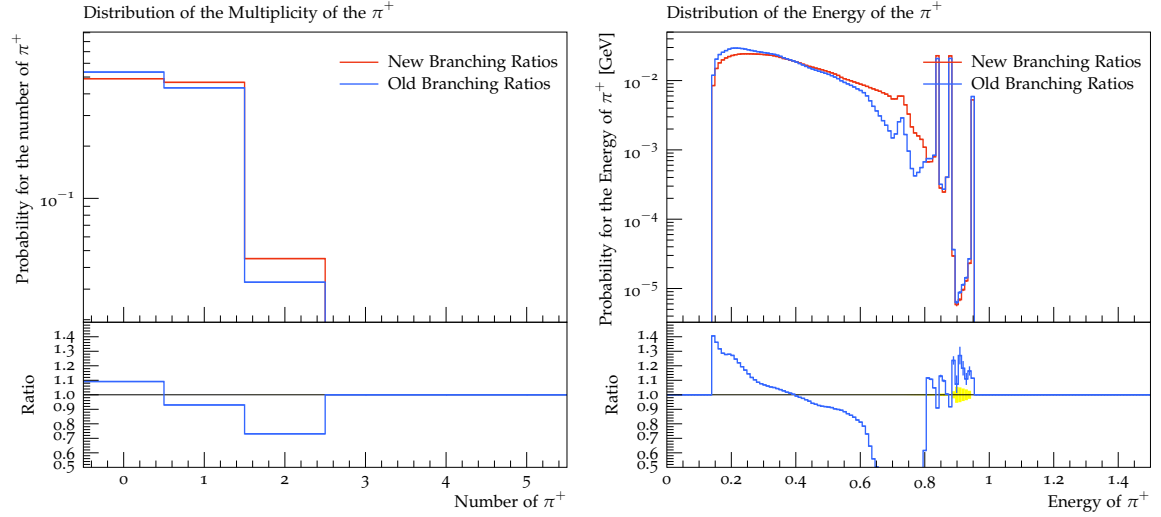
Figure 4.3: multiplicity and energy spectrum of the π^+

and

$$\Lambda_c^+ \to \Sigma + \pi^+.$$

In these processes one π^+ is created and both branching ratios has been increased. This explains the increase of the probability for the production of on pion.

The decay channel

$$\Lambda_c^+ \to \Sigma^- + \pi^+ + \pi^+$$

was added to the decay table. This process leads to the increase of the probability for pion multiplicity two.

The new decay channel

$$\Lambda_c^+ \to \Lambda + \pi^+ + \pi$$

is the reason why the gap near 0.7 GeV is filled. It is the only reason for this change because in 4.9 happens the same thing for the π. And the only new process with a π^+ and a π in the final state is the process

$$\Lambda_c^+ \to \Lambda + \pi^+ + \pi$$

The peaks in the energy spectrum can be identified with specific decay channels. This channels are $1 \to 2$ processes because in such a process the dynamics of the end products is well determined due to momentum conversation. The peak with the highest energy is obtained

from

$$\Lambda_c^+ \to n + \pi^+$$

because the proton have the lowest mass from all products of $1 \to 2$ processes with a π^+ in the final state. The second peak comes from

$$\Lambda_c^+ \to \Lambda + \pi^+,$$

the third from

$$\Lambda_c^+ \to \Sigma + \pi^+$$

and the fourth from

$$\Lambda_c^+ \to \Delta(1232) + \pi^+.$$

The peak from the $\Delta(1232)$ is at the lowest postion because the mass of this particle is the highest compared to the others.
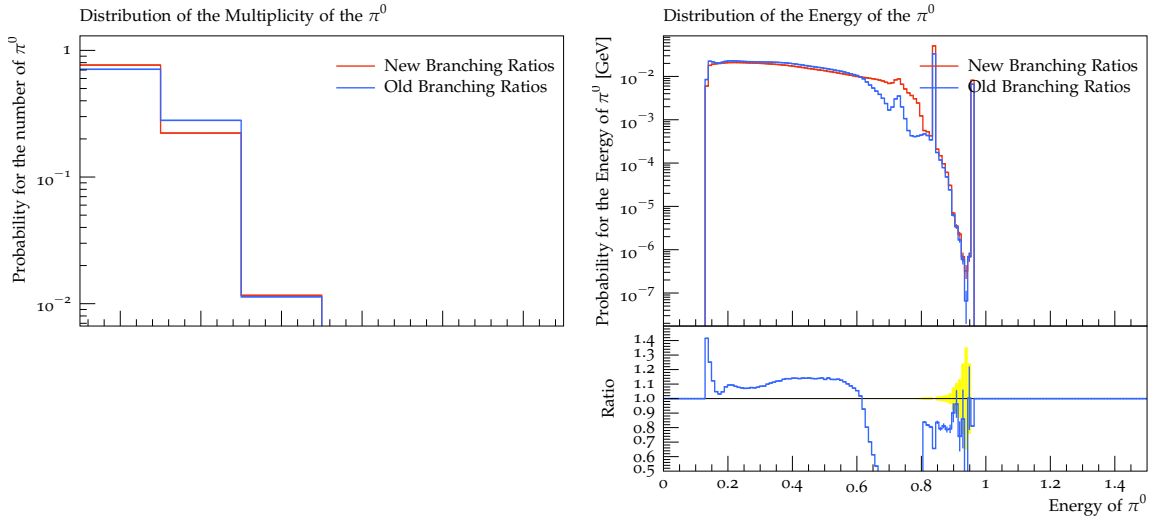
Figure 4.4: multiplicity and energy spectrum of the π

The diagram 4.9 is very similar to 4.3. For a complete decay chain A.3 the distribution for the π disappears because it is unstable.

In the further consideration only the other end product for $1 \to 2$ process that leads to a peak is used to characterize the decay. This is simpler and the other end product will always be the regarded particle of the energy spectrum. The other end product besides the π has to be a positive charged particle. The family of baryons for the decay will be the same only a charged particle is picked up. For the Λ baryons exist only the Λ_t^+ besides the Λ_c^+ with a positive charge. Both are no decay candidates because their masses are to high. So at this position

there will be no peak. The peaks from the right to the left results from the following decays: n, Σ^+, $\Delta(1232)^+$. The diagram 4.5 show only little changes. No decay channels with a K^+
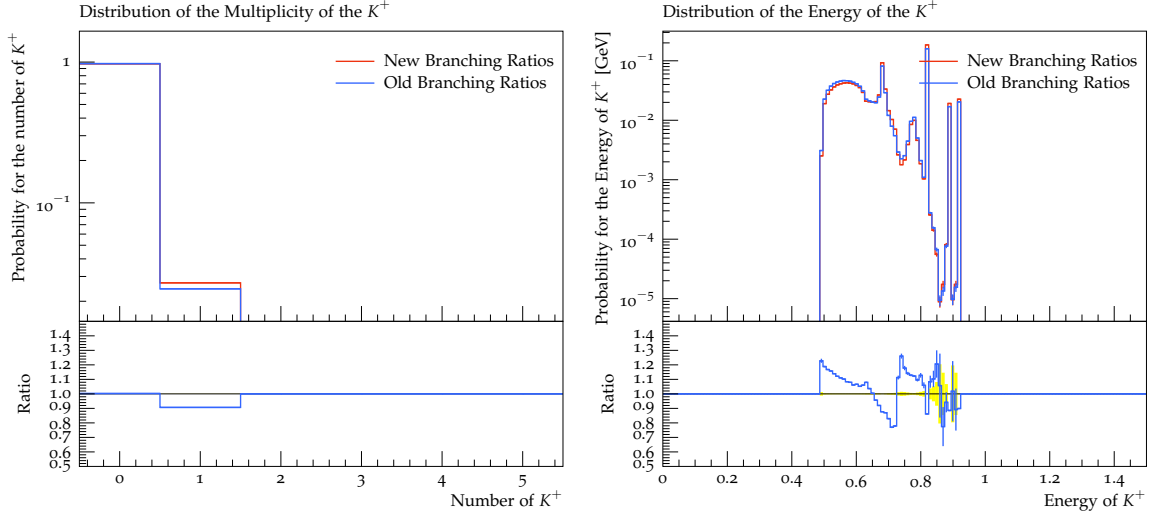
Figure 4.5: multiplicity and energy spectrum of the K^+

in the final state were added and so this result is aspected. Due to the masses of the other particle in the final state the peaks can be connected to the different decay channels. From right to the left the peaks results from $1 \to 2$ decays with a Λ, Σ, Ξ, $\Sigma(1385)$ or a $\Xi(1530)$ and a K^+ in the final state. The events that are missed in 4.6 are in 4.7 because the process
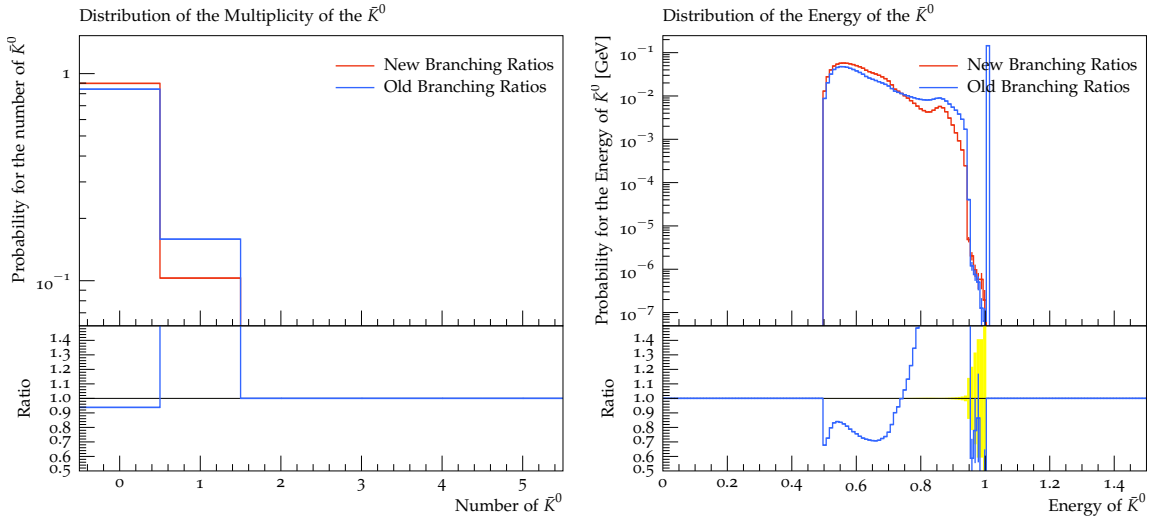
Figure 4.6: multiplicity and energy spectrum of the $\bar{K}$

$$\Lambda_c^+ \to P^+ + K_b$$

was changed to

$$\Lambda_c^+ \to P^+ + K_s$$
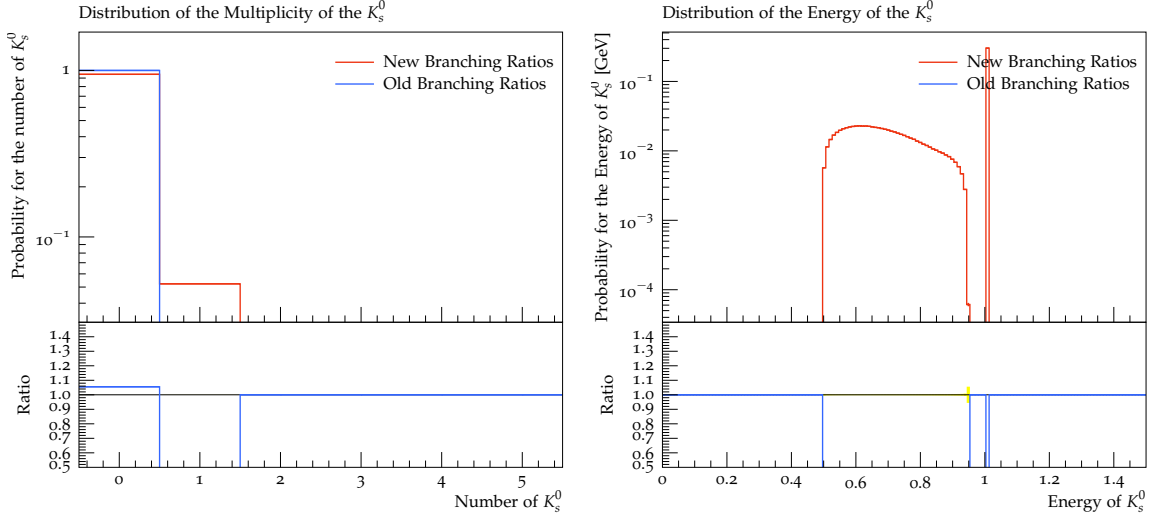
Figure 4.7: multiplicity and energy spectrum of the K_s

. The process

$$\Lambda_c^+ \rightarrow P^+ + K_s + \pi^+ + \pi^-$$

was added as a decay channel. This leads to the distribution in the two diagrams. The peak in 4.7 belongs to the proton. The $1 \rightarrow 2$ decays with a Σ^+ is the reason for the high isolated
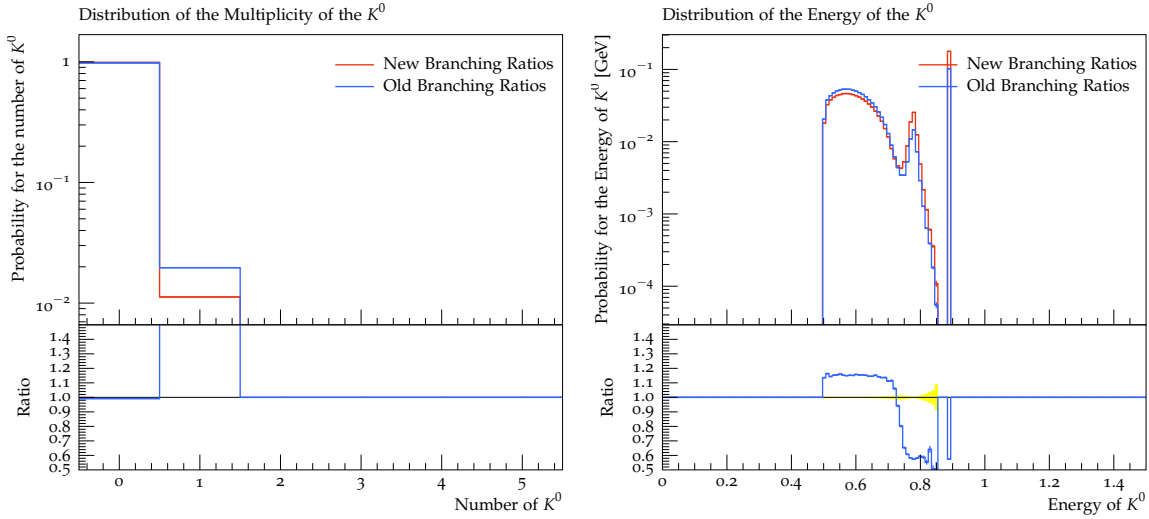
Figure 4.8: multiplicity and energy spectrum of the K

peak and $\Sigma(1385)+$ for the peak on the hill. The diagrams are changed slightly because the branching ratios were changed. They were decreased. The decrease of the process

$$\Lambda_c^+ \rightarrow P^+ + \pi^+ + \pi^+ + \pi^- + \pi^-$$

has an dramatically impact of the multiplicity diagram because it is the only process that produces two π^-. The red bulge is a superposition of all little changes because no processes
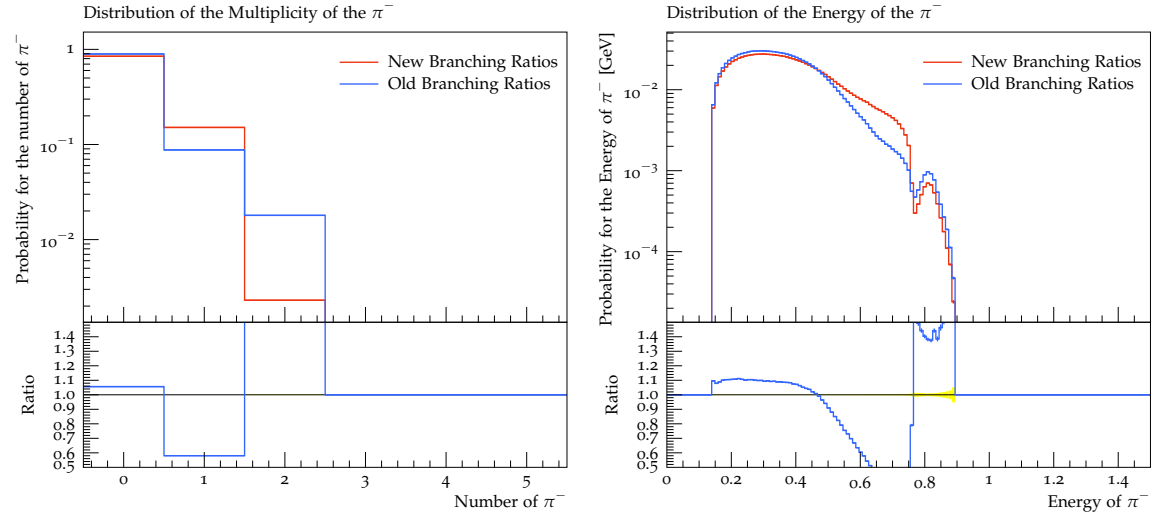
Figure 4.9: multiplicity and energy spectrum of the π^-

were changed so drastically.

4.2 Form Factor Models

All diagrams of the form factors show the same behavior, there is no difference in the semilep-
tonic decays in electron or muon except of the cut-off due to the higher muon mass compared
to the elecron mass. So the figures for the electrons were used in the following sections.
The goal of this section is to find the best form factor model that fits the experimental results
4.10 from the CLEO II detector[3]. The CLEO II detector has measured the $\Lambda_c^+ \to \Lambda + e^+ + \nu_e$
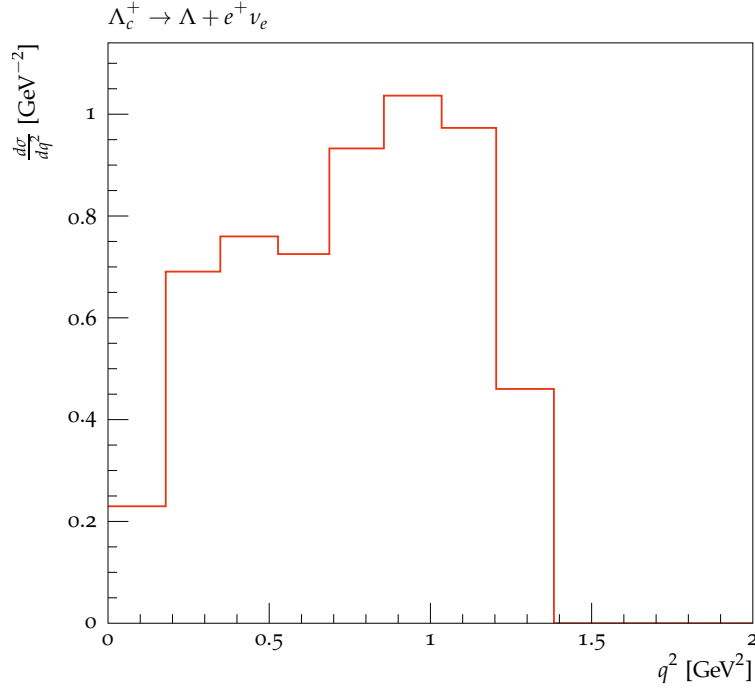
Figure 4.10: Experimental results from the CLEO II detector for the $\Lambda_c^+ \to \Lambda + e^+ + \nu_e$
decay

decay channel. The observables for the comparison have to be defined first.

4.2.1 Observables

Two observables are adapted from simulations of the `BELLE` experiment to compare the different
form factors. The first is q^2 which is defined as

$$q^2 = (p_{\Lambda_c} - p_B)^2 \, a \tag{4.1}$$

and the second is the recoil of the W boson:

$$w = \frac{p_{\Lambda_c}^2 + p_B^2 - (p_{\Lambda_c} - p_B)^2}{2 \cdot \sqrt{p_{\Lambda_c}^2} \cdot \sqrt{p_B^2}}. \tag{4.2}$$

The experimental data use the first observable (4.1). So only this one will be compared. The figures for the recoil of the W boson can be found in the appendixA.4

4.2.2 Previous form factor models
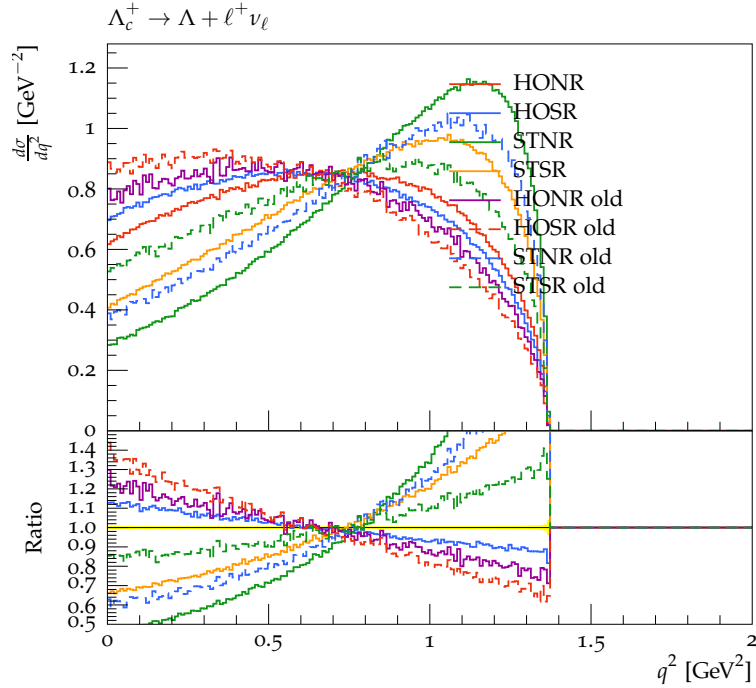
Figure 4.11: Comparison from the already implemented form factor models in leadding order (old) and with all factors for Λ

For the Λ_c^+ alrady exists four form factor models. The harmonic oszillator non relativistic (HONR), the harmonic oszillator semi relativistic (HOSR), the sturmian non relativistic (STNR) and the the sturmian semi relativistic (STSR) model. Harmonic oszillator and sturmian are to different expansion bases for the wave function. [14]

But for this models only the first form factor were used to calculate the transition matrix. These are the lines that marked with old. The other four lines are made with the whole number of form factors. You can see that the shape of the curves with only one form factor are more flat compared to the curves with all form factors. So all form factors have a not neglectable influence to the transistion matrix element and the leading order term is not enough for the simulation.

For the following form factor models all form factors are used to get accurate results.

4.2.3 $\Lambda_c^+ \to \Lambda + l^+ + \nu_l$
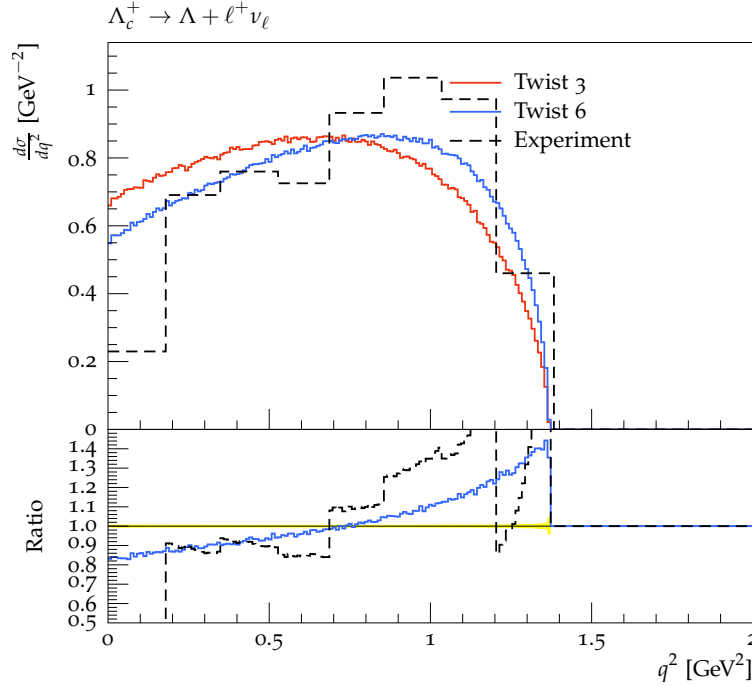
Figure 4.12: Comparison from the different parametrization of the LCSR model for Λ

The both parametrizations of the light-cone sum rule in 4.12 for different twist show similar properties. You can see that this model did not fit the experimental results.

Triangular and Rectangular are different continuums models in figure 4.13 used by the QCD sum rule model and the number is the value of κ. This is an parameter of the parametrization. The behavior of the QCD sum rule model in 4.13 is very different for the two classes of parametrizations, Pole and Full. The pole parametrizations themselves are very similar. They only have little deviations to each other. The general behavior of the pole parametrizations is flat and has no thin maximum.

The full parametrizations on the other hand have a clear maxmimum and a more steep slope. The full parametrization with the continuums model triangular and $\kappa = 2$ is an exception. The full parametrizations in the rectangular continuums model are very close and a dstinction is not possible.

The diagram 4.14 shows the big differences between the different models. The spread between the curves is very high. The CCQM and the RQM are very similar. The QCDSR model with triangular continuums model and $\kappa = 2$ fits the experimental data best.

In (4.15) is a comparison with the original implemented form factor models. The LCS is similar to the HONR.
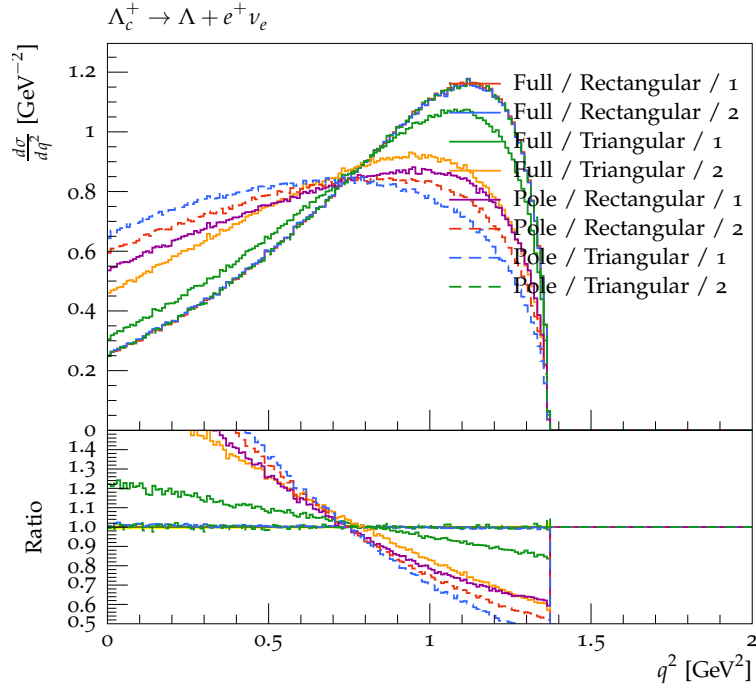
Figure 4.13: Comparison from the different parametrization of the QCDSR model for Λ

The STSR fits the measurement also well. But the first bin is not matching very well and also the maximum is to low.

So the model that fits the decay $\Lambda_c^+ \rightarrow \Lambda + l^+ + \nu_l$ the best is the QCDSR model with triangular continuums model and $\kappa = 2$.
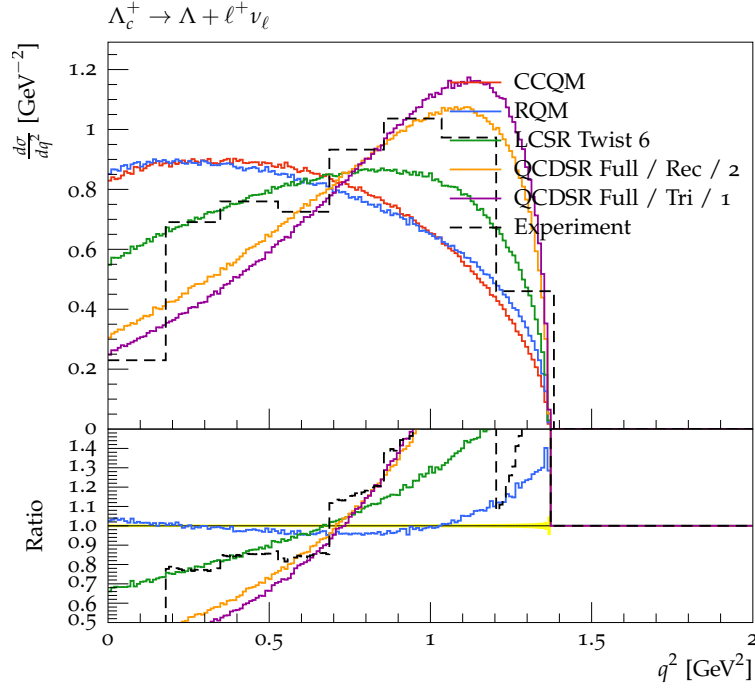
Figure 4.14: Comparison from some of the self implemented form factor models for Λ
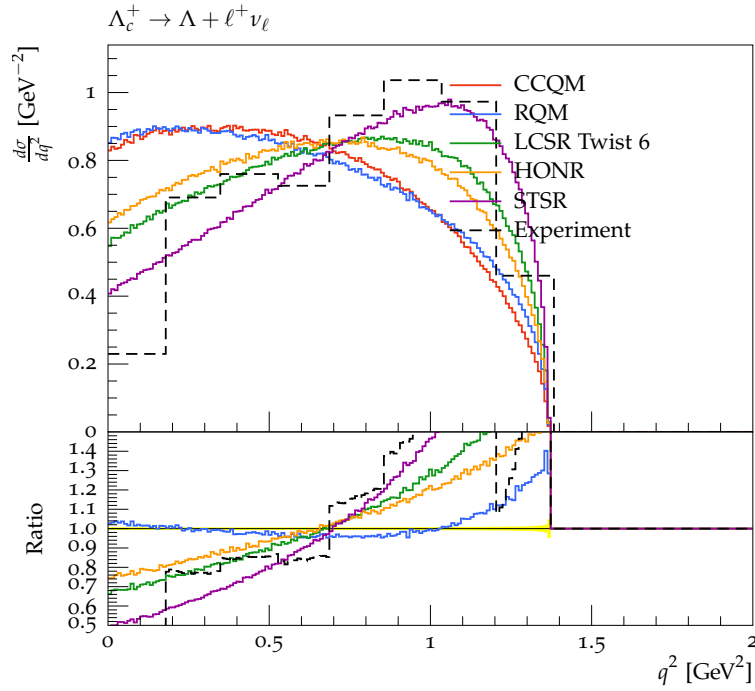
Figure 4.15: Comparison from the already implemented form factor models with some of the self implemented ones for Λ

4.2.4 $\Lambda_c^+ \to n + l^+ + \nu_l$
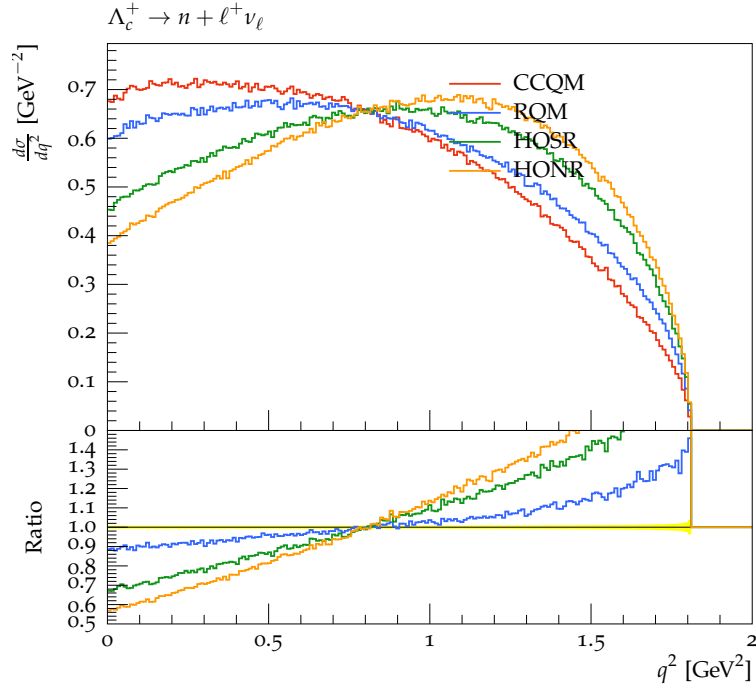
Figure 4.16: Comparison from the already implemented form factor models with the self implemented ones for the neutron

The form factor models 4.16 shows in general a more flat shape compared to the results for the $\Lambda_c^+ \to \Lambda + l^+ + \nu_l$ decay. Only the CCQM and the RQM have an computation for the neutron. The already implemented HOSR was also used. No experimental data exists for this decay.

The models for the neutron didn't have such big deviations like the ones for the Λ. So the choice of the model is not so important for the neutron because all of this will give similar results due to the similar shape.

5 Summary and Outlook

The non relativistic quak model [11] was introduced and implemented with this thesis in `Sherpa` but not tested becau for the exicted Λ states not so much experimental data exists. This model could be tested and verified. An implementation of the form factor model from Lattice QCD [12] would be a great work. The Lattice QCD is a modern method of the QCD and used in many aspect. So the result from this form factor model would be very interesting.

6 Bibliography

[1] R. S. Marques de Carvalho et al. "Form factors and decay rates for heavy Λ semileptonic decays from QCD sum rules". In: *Phys. Rev. D* 60 (3 1999), p. 034009. DOI: 10.1103/PhysRevD.60.034009. URL: https://link.aps.org/doi/10.1103/PhysRevD.60.034009.

[2] A. Ceccucci (CERN), Z. Ligeti (LBNL), and Y. Sakai (KEK). *THE CKM QUARK-MIXING MATRIX*. 2016. URL: http://pdg.lbl.gov/2016/reviews/rpp2016-rev-ckm-matrix.pdf (visited on 03/27/2017).

[3] G. Crawford et al. "Form Factor Ratio Measurement in $\Lambda_c^+ \to \Lambda e^+ \nu_e$". In: *Phys. Rev. Lett.* 75 (4 1995), pp. 624–628. DOI: 10.1103/PhysRevLett.75.624. URL: https://link.aps.org/doi/10.1103/PhysRevLett.75.624.

[4] C. Patrignani et al.(Particle Data Group). *CHARMED BARYONS Λ_c^+*. 2016. URL: http://pdglive.lbl.gov/Particle.action?node=S033&init= (visited on 03/09/2017).

[5] R. N. Faustov and V. O. Galkin. "Semileptonic decays of Λ_b baryons in the relativistic quark model". In: *Phys. Rev. D* 94 (7 2016), p. 073008. DOI: 10.1103/PhysRevD.94.073008. URL: https://link.aps.org/doi/10.1103/PhysRevD.94.073008.

[6] R. N. Faustov and V. O. Galkin. "Semileptonic decays of Λ_c baryons in the relativistic quark model". In: *Eur. Phys. J.* C76.11 (2016), p. 628. DOI: 10.1140/epjc/s10052-016-4492-z. arXiv: 1610.00957 [hep-ph].

[7] T. Gleisberg et al. "Event generation with SHERPA 1.1". In: *JHEP* 02 (2009), p. 007. DOI: 10.1088/1126-6708/2009/02/007. arXiv: 0811.4622 [hep-ph].

[8] Thomas Gutsche et al. "Heavy-to-light semileptonic decays of Λ_b and Λ_c baryons in the covariant confined quark model". In: *Phys. Rev.* D90.11 (2014). [Erratum: Phys. Rev.D94,no.5,059902(2016)], p. 114033. DOI: 10.1103/PhysRevD.90.114033,10.1103/PhysRevD.94.059902. arXiv: 1410.6043 [hep-ph].

[9] Thomas Gutsche et al. "Semileptonic decays $\Lambda_c^+ \to \Lambda \ell^+ \nu_\ell \ (\ell = e, \mu)$ in the covariant quark model and comparison with the new absolute branching fraction measurements of Belle and BESIII". In: *Phys. Rev.* D93.3 (2016), p. 034008. DOI: 10.1103/PhysRevD.93.034008. arXiv: 1512.02168 [hep-ph].

[10]   Ming-Qiu Huang and Dao-Wei Wang. "Semileptonic decay Lambda(c) —> Lambda l+ nu from QCD light-cone sum rules". In: (2006). arXiv: `hep-ph/0608170 [hep-ph]`.

[11]   Md Mozammel Hussain and Winston Roberts. "Λ_c Semileptonic Decays in a Quark Model". In: *Phys. Rev.* D95.5 (2017). [Addendum: Phys. Rev.D95,no.9,099901(2017)], p. 053005. DOI: `10.1103/PhysRevD.95.099901,10.1103/PhysRevD.95.053005`. arXiv: `1701.03876 [nucl-th]`.

[12]   Stefan Meinel. "$\Lambda_c \to \Lambda l^+\nu_l$". In: *Phys. Rev. Lett.* 118 (8 2017), p. 082001. DOI: `10.1103/PhysRevLett.118.082001`. URL: `https://link.aps.org/doi/10.1103/PhysRevLett.118.082001`.

[13]   Muslema Pervin, Winston Roberts, and Simon Capstick. "Semileptonic decays of heavy lambda baryons in a quark model". In: *Phys. Rev.* C72 (2005), p. 035201. DOI: `10.1103/PhysRevC.72.035201`. arXiv: `nucl-th/0503030 [nucl-th]`.

[14]   Muslema Pervin, Winston Roberts, and Simon Capstick. "Semileptonic decays of heavy lambda baryons in a quark model". In: *Phys. Rev.* C72 (2005), p. 035201. DOI: `10.1103/PhysRevC.72.035201`. arXiv: `nucl-th/0503030 [nucl-th]`.

[15]   Frank Siegert. "Simulation of hadron decays in SHERPA". In: (2007).

A Appendix

A.1 Decays.dat

Table A.1: Full list of changes in the Decays.dat from the Λ_c^+

Status	Outgoing Part.	BR(Delta BR)[Origin]	Decay
Modes with nucleons/Deltas			
old	2212,-311	0.023(0.006)[PDG]	$\Lambda_c^+ \to P^+ + K_b$
new	2212,310	0.0158(0.0008)[PDG]	$\Lambda_c^+ \to P^+ + K_s$
old	2212,-313	0.016(0.005)[PDG]	$\Lambda_c^+ \to P^+ + K^*(892)_b$
new	2212,-313	0.0198(0.0028)[PDG]	
old	2212,-321,211	0.028(0.008)[PDG]	$\Lambda_c^+ \to P^+ + K^- + \pi^+$
new	2212,-321,211	0.035(0.004)[PDG]	
old	2212,-311,111	0.033(0.010)[PDG]	$\Lambda_c^+ \to P^+ + K_b + \pi$
new	2212,310,111	0.0199(0.0013)[PDG]	
old	2212,-311,221	0.012(0.004)[PDG]	$\Lambda_c^+ \to P^+ K_b + \eta$
new	2212,-311,221	0.016(0.004)[PDG]	
old	2212,-311,211,-211	0.026(0.007)[PDG]	$\Lambda_c^+ \to P^+ + K_b + \pi^+ + \pi^-$
new	2212,-311,211,-211	0.049(0.004)[PDG]	
created	2212,310,211,-211	0.0166(0.0012)[PDG]	$\Lambda_c^+ \to P^+ + K_s + \pi^+ + \pi^-$
old	2212,-323,211	0.016(0.005)[PDG]	$\Lambda_c^+ \to P^+ + K^*(892)_b^+ + \pi^+$
new	2212,-323,211	0.015(0.005)[PDG]	
old	2212,-321,211,111	0.036(0.012)[PDG]	$\Lambda_c^+ \to P^+ + K^- + \pi^+ + \pi$
new	2212,-321,211,111	0.046(0.09)[PDG]	
old	2212,-321,211,211,-211	0.0011(0.0008)[PDG]	$\Lambda_c^+ \to P^+ + K^- + \pi^+ + \pi^+ + \pi^-$
new	2212,-321,211,211,-211	0.0014(0.001)[PDG]	
old	2212,-321,211,111,111	0.008(0.004)[PDG]	$\Lambda_c^+ \to P^+ + K^- + \pi^+ + \pi + \pi$
new	2212,-321,211,111,111	0.01(0.005)[PDG]	
old	2212,333	0.00082(0.00027)[PDG]	$\Lambda_c^+ \to P^+ + \phi(1020)$
new	2212,333	0.00104(0.00021)[PDG]	
S = 0			

old	2212,321,-321	0.00035(0.00017)[PDG]	$\Lambda_c^+ \to P^+ + K^+ + K^-$
new	2212,321,-321	0.00044(0.00018)[PDG]	
S = 0			
old	2212,211,211,-211,-211	0.018(0.012)[PDG]	$\Lambda_c^+ \to P^+ + \pi^+ + \pi^+ + \pi^- + \pi^-$
new	2212,211,211,-211,-211	0.0023(0.0015)[PDG]	
S = 0			
old	2212,9010221	0.0028(0.0019)[PDG]	$\Lambda_c^+ \to P^+ + f(0980)$
new	2212,9010221	0.0035(0.0023)[PDG]	
S = 0			
deleted	2212,211,-211	0.0007(0.0007)[PDG]	$\Lambda_c^+ \to P^+ + \pi^+ + \pi^-$
S = 0			
old	2224,-321	0.0086(0.003[PDG]	$\Lambda_c^+ \to \Delta(1232)^{++} + K^-$
new	2224,-321	0.0109(0.0025)[PDG]	
Modes with hyperons			
old	3122,211	0.0107(0.0028)[PDG]	$\Lambda_c^+ \to \Lambda + \pi^+$
new	3122,211	0.0130(0.0007)[PDG]	
created	3122,211,111	0.071(0.0004)[PDG]	$\Lambda_c^+ \to \Lambda + \pi^+ + \pi$
created	3122,213	0.036(0.013)[PDG]	$\Lambda_c^+ \to \Lambda + \rho(770)^+$
S = 0			
old	3122,321	0.0005(0.00016)[PDG]	$\Lambda_c^+ \to \Lambda + K^+$
new	3122,321	0.00061(0.00012)[PDG]	
old	3122,211,113	0.011(0.005)[PDG]	$\Lambda_c^+ \to \Lambda + \pi^+ + \rho(770)$
new	3122,211,113	0.015(0.006)[PDG]	
old	3122,221,211	0.018(0.006)[PDG]	$\Lambda_c^+ \to \Lambda + \eta + \pi^+$
new	3122,221,211	0.022(0.005)[PDG]	
old	3122,223,211	0.018(0.006)[PDG]	$\Lambda_c^+ \to \Lambda + \omega(782) + \pi^+$
new	3122,223,211	0.015(0.005)[PDG]	
old	3122,321,-311	0.0047(0.0015)[PDG]	$\Lambda_c^+ \to \Lambda + K^+ + K_b$
new	3122,321,-311	0.0057(0.0011)[PDG]	
old	3114,211,211	0.0055(0.0017)[PDG]	$\Lambda_c^+ \to \Sigma(1385)^- + \pi^+ + \pi^+$
new	3114,211,211	0.0090(0.0018)[PDG]	
created	3112,211,211	0.021(0.004)[PDG]	$\Lambda_c^+ \to \Sigma^- + \pi^+ + \pi^+$
old	3212,211	0.0105(0.0028)[PDG]	$\Lambda_c^+ \to \Sigma + \pi^+$
new	3212,211	0.0129(0.0007)[PDG]	
S = 0			
old	3212,321	0.00042(0.00013)[PDG]	$\Lambda_c^+ \to \Sigma + K^+$

new	3212,321	0.00052(0.00008)[PDG]	
old	3212,211,211,-211	0.0083(0.0031)[PDG]	$\Lambda_c^+ \to \Sigma + \pi^+ + \pi^+ + \pi^-$
new	3212,211,211,-211	0.0113(0.0029)[PDG]	
old	3222,111	0.0100(0.0034)[PDG]	$\Lambda_c^+ \to \Sigma^+ + \pi$
new	3222,111	0.0124(0.001)[PDG]	
old	3222,221	0.0055(0.0023)[PDG]	$\Lambda_c^+ \to \Sigma^+ + \eta$
new	3222,221	0.0070(0.0023)[PDG]	
old	3222,211,-211	0.013(0.005)[PDG]	$\Lambda_c^+ \to \Sigma^+ + \pi^+ + \pi^-$
new	3222,211,-211	0.0457(0.0029)[PDG]	
S = 0			
old	3222,313	0.002[EvtGen]	$\Lambda_c^+ \to \Sigma^+ + K^*(892)$
new	3222,313	0.0036(0.001)[PDG]	
old	3222,223	0.027(0.01)[PDG]	$\Lambda_c^+ \to \Sigma^+ + \omega(782)$
new	3222,223	0.0174(0.0021)[PDG]	
old	3222,333	0.0031(0.0009)[PDG]	$\Lambda_c^+ \to \Sigma^+ + \phi(1020)$
new	3222,333	0.0040(0.0006)[PDG]	
old	3224,113	0.0037(0.0031)[PDG]	$\Lambda_c^+ \to \Sigma(1385)^+ + \rho(770)$
new	3224,113	0.0072(0.0046)[PDG]	
old	3224,221	0.0085(0.0033)[PDG]	$\Lambda_c^+ \to \Sigma(1385)^+ + \eta$
new	3224,221	0.00124(0.00037)[PDG]	
old	3224,211,-211	0.007(0.004)[PDG]	$\Lambda_c^+ \to \Sigma(1385)^+ + \pi^+ + \pi^-$
new	3224,211,-211	0.011(0.006)[PDG]	
old	3322,321	0.0039(0.0014)[PDG]	$\Lambda_c^+ \to \Xi + K^+$
new	3322,321	0.0050(0.0012)[PDG]	
old	3312,321,211	0.0025(0.001)[PDG]	$\Lambda_c^+ \to \Xi^- + K^+ + \pi^+$
new	3312,321,211	0.0062(0.0006)[PDG]	
old	3324,321	0.0026(0.001)[PDG]	$\Lambda_c^+ \to \Xi(1530) + K^+$
new	3324,321	0.0033(0.0009)[PDG]	
semileptonic modes			
old	3122,12,-11	0.021(0.006)[PDG]	$\Lambda_c^+ \to \Lambda + \nu_e + e^+$
new	3122,12,-11	0.036(0.004)[PDG]	
old	3122,14,-13	0.020(0.007)[PDG]	$\Lambda_c^+ \to \Lambda + \nu_\mu + \mu^+$
new	3122,14,-13	0.036(0.004)[PDG]	

A.2 Primary Decays
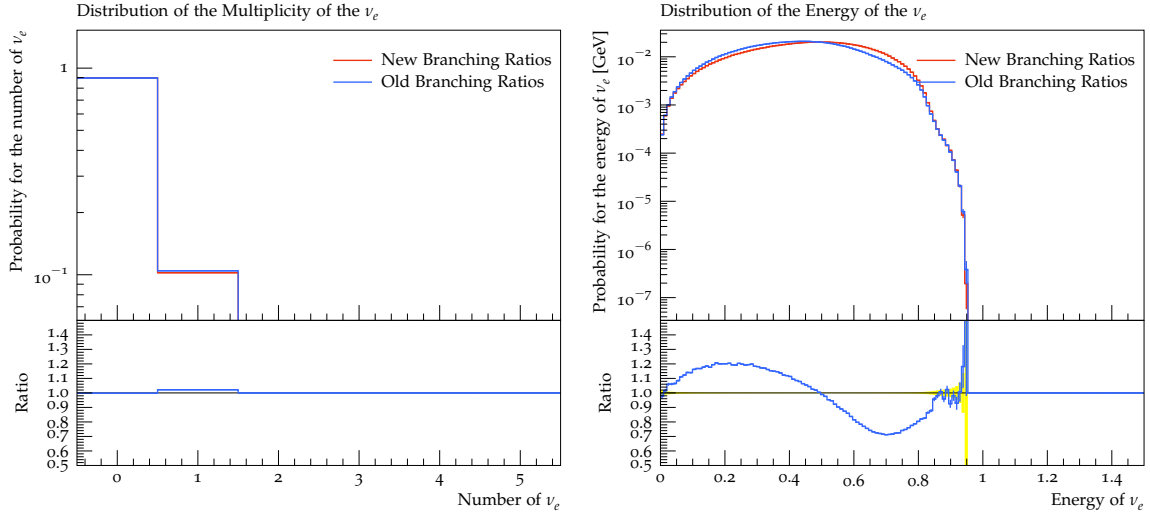
Figure A.1: multiplicity and energy spectrum of the ν_e
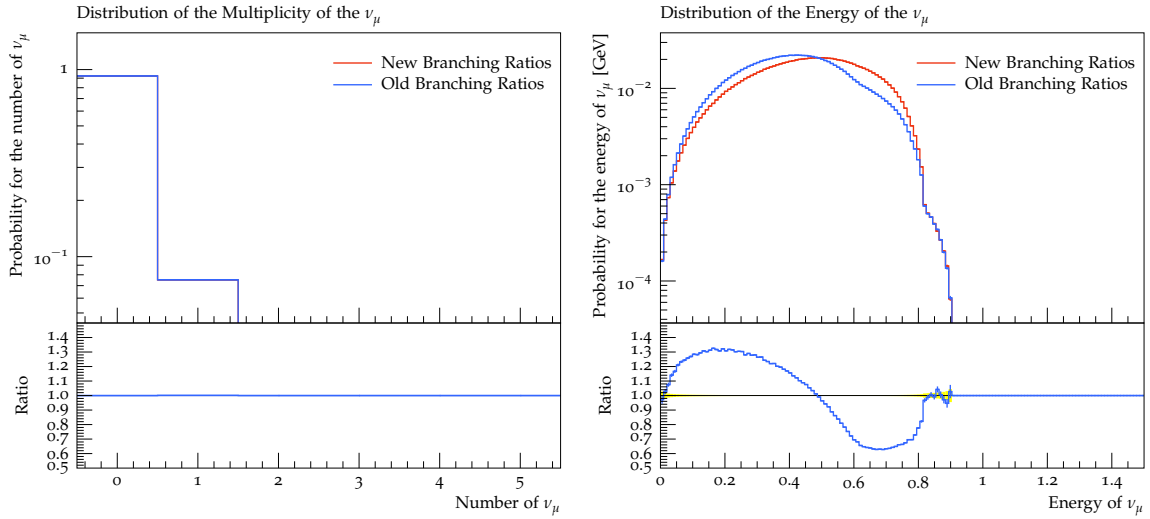
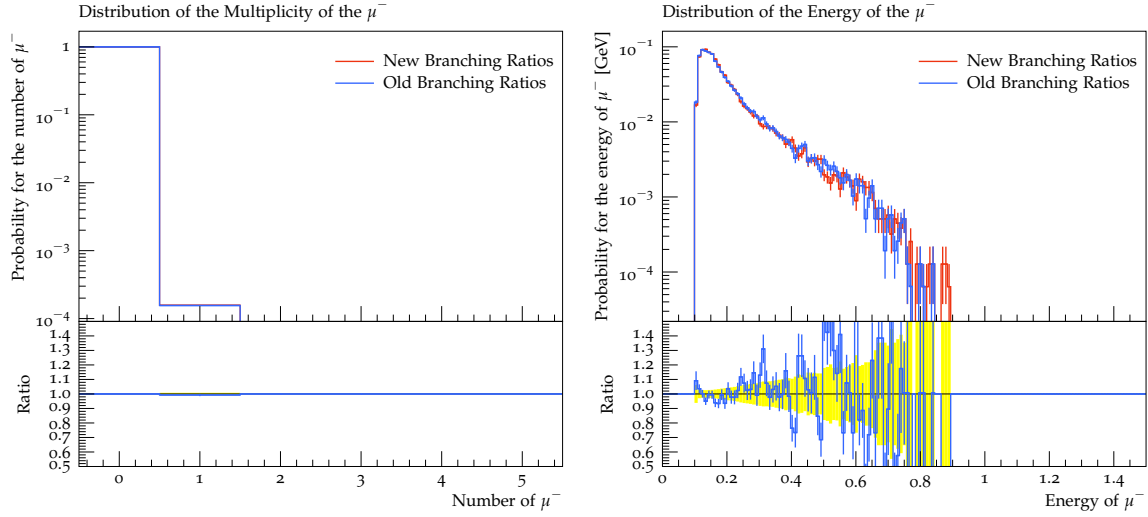**Figure A.2:** multiplicity and energy spectrum of the ν_μ
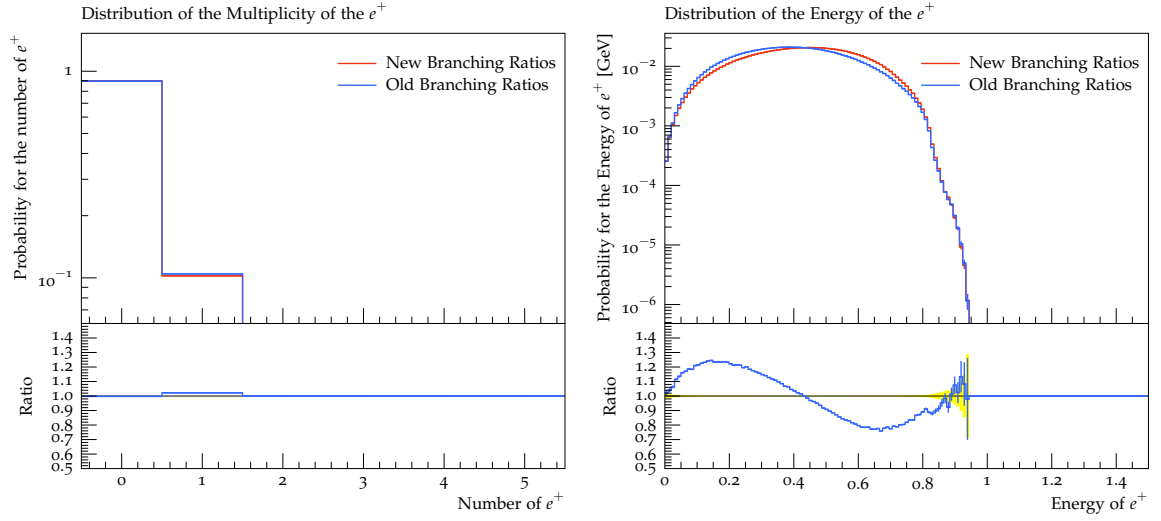
Figure A.3: multiplicity and energy spectrum of the e^+
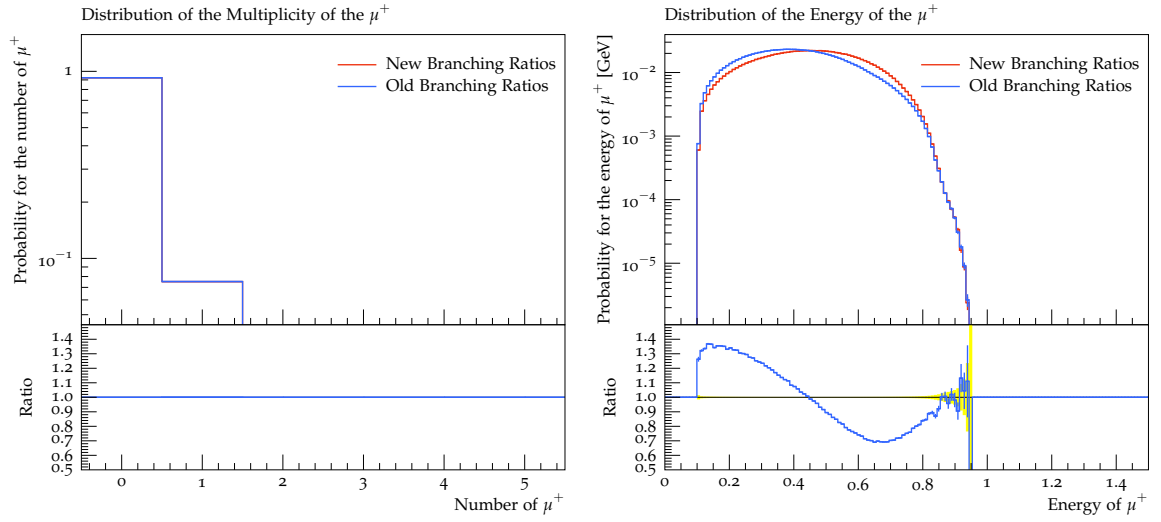
Figure A.4: multiplicity and energy spectrum of the μ^+
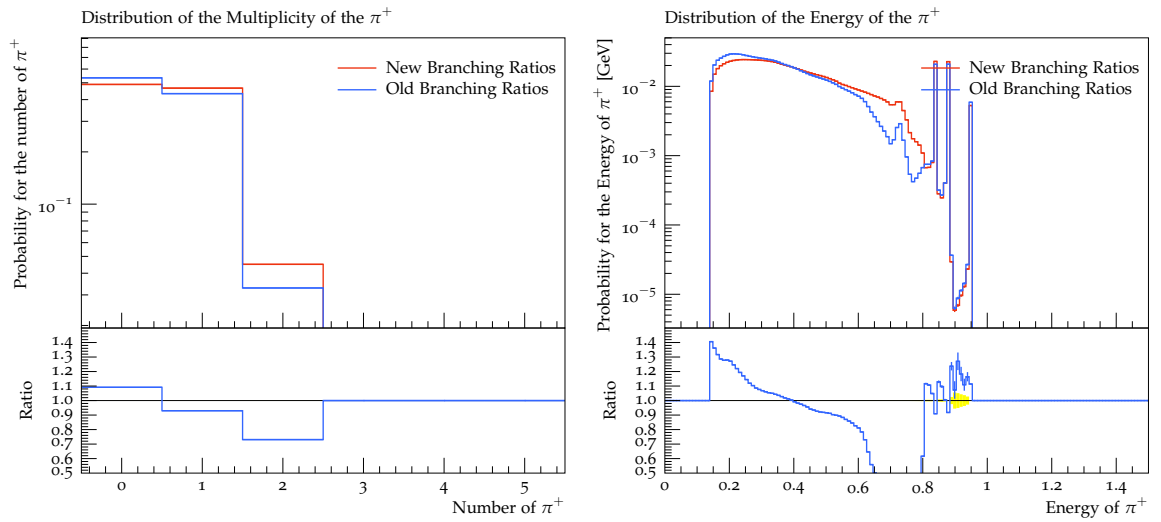
Figure A.5: multiplicity and energy spectrum of the π^+
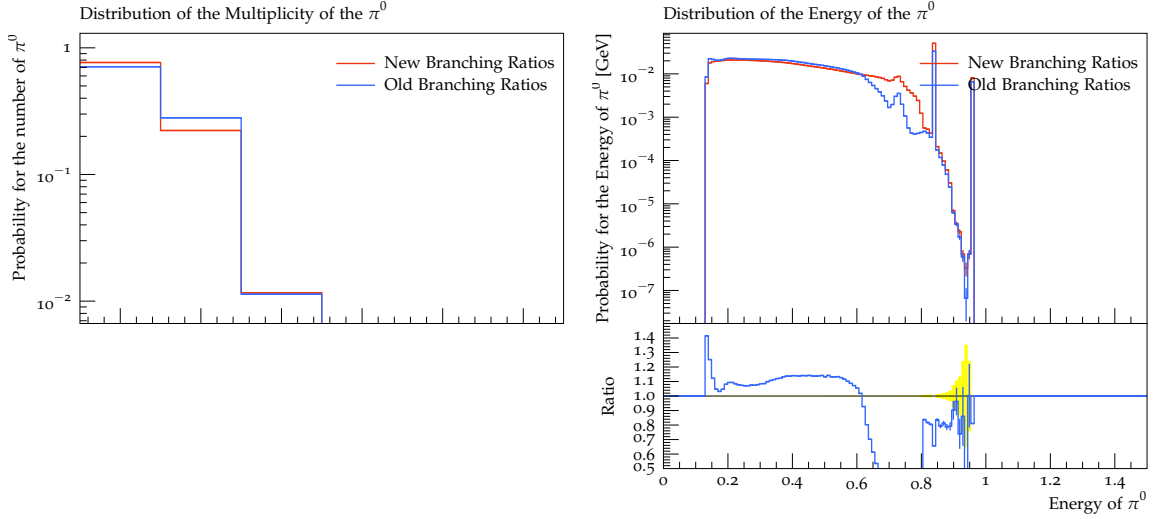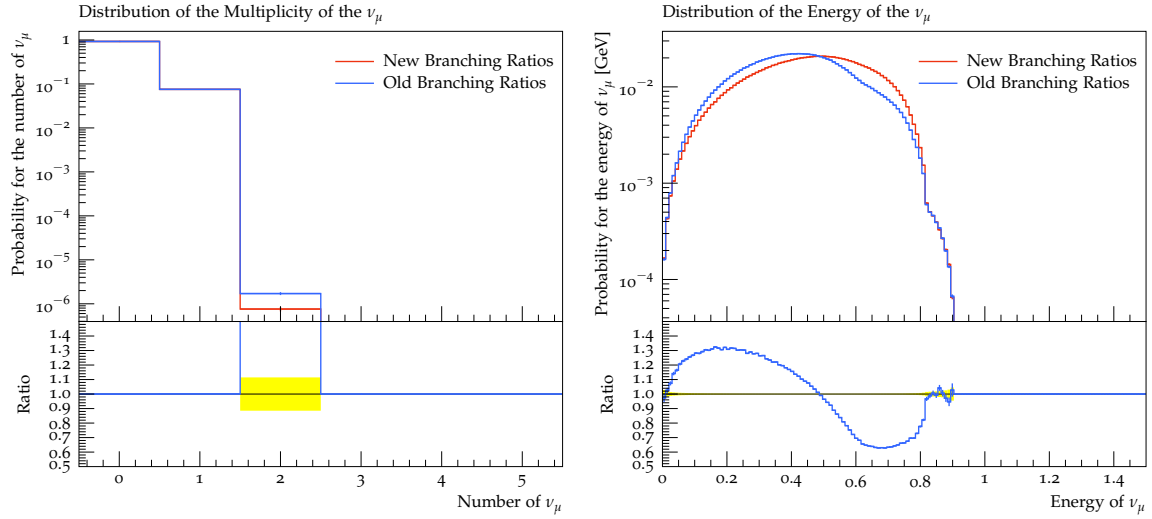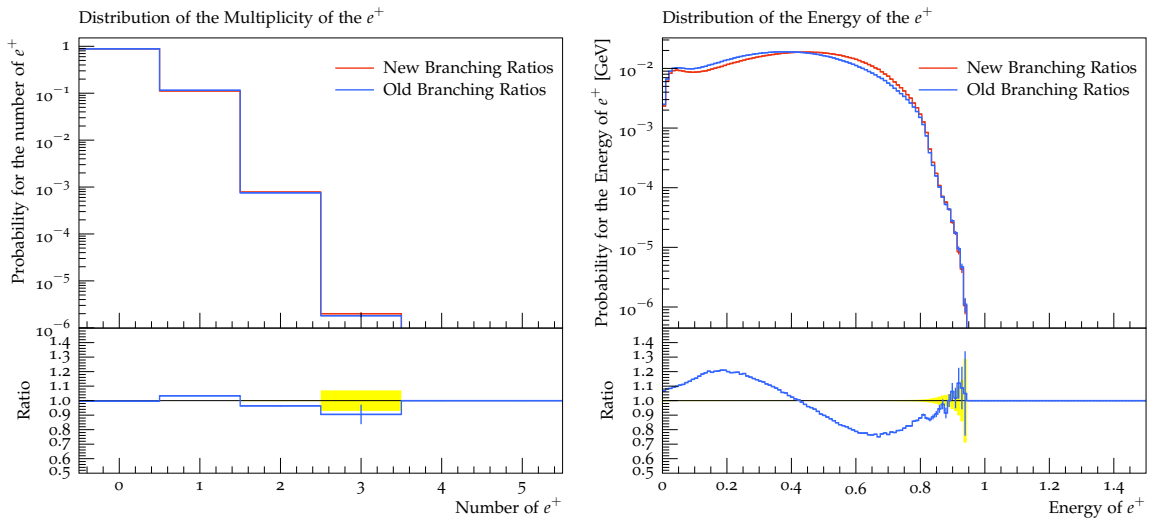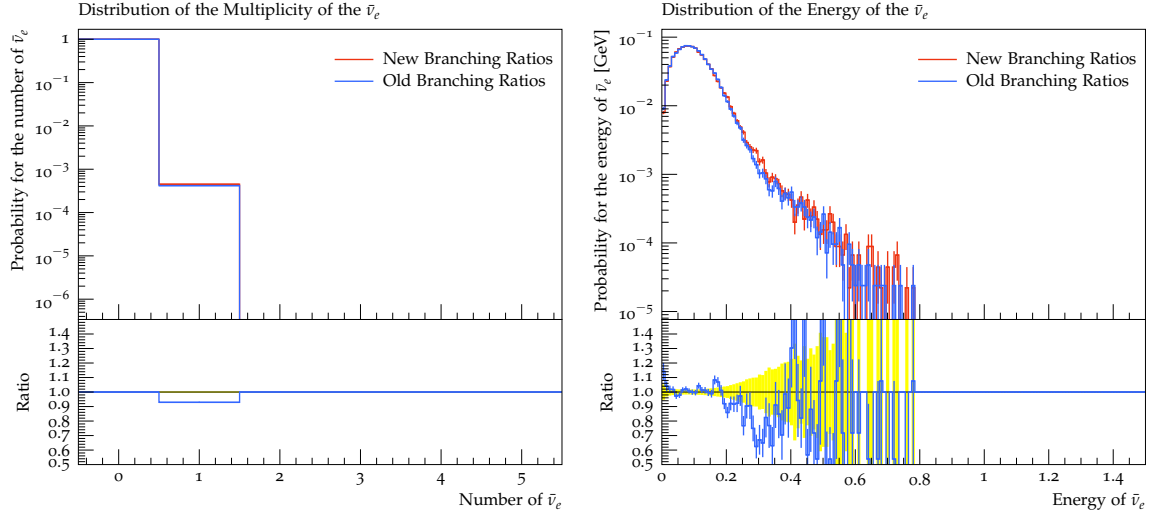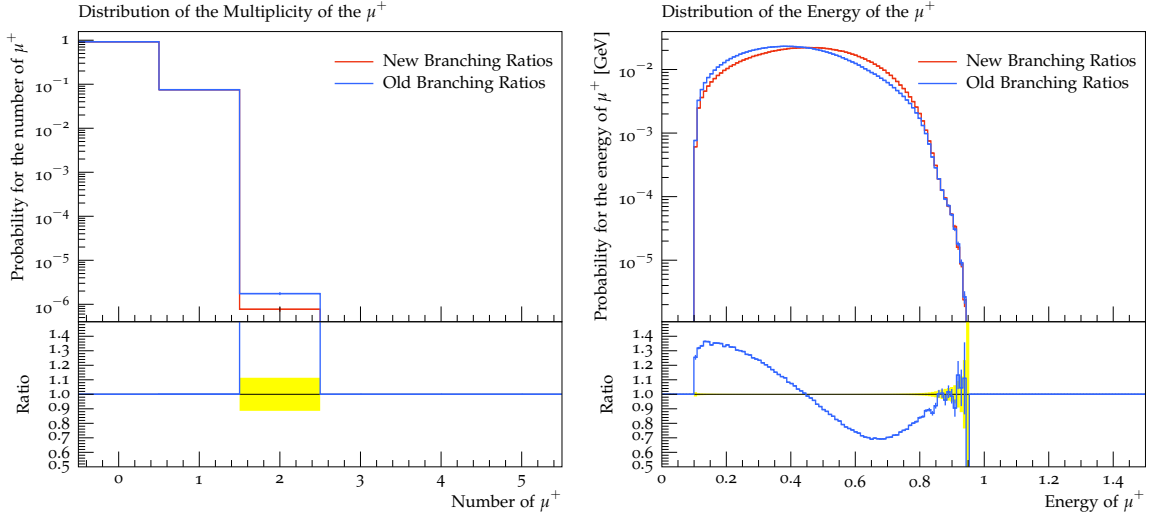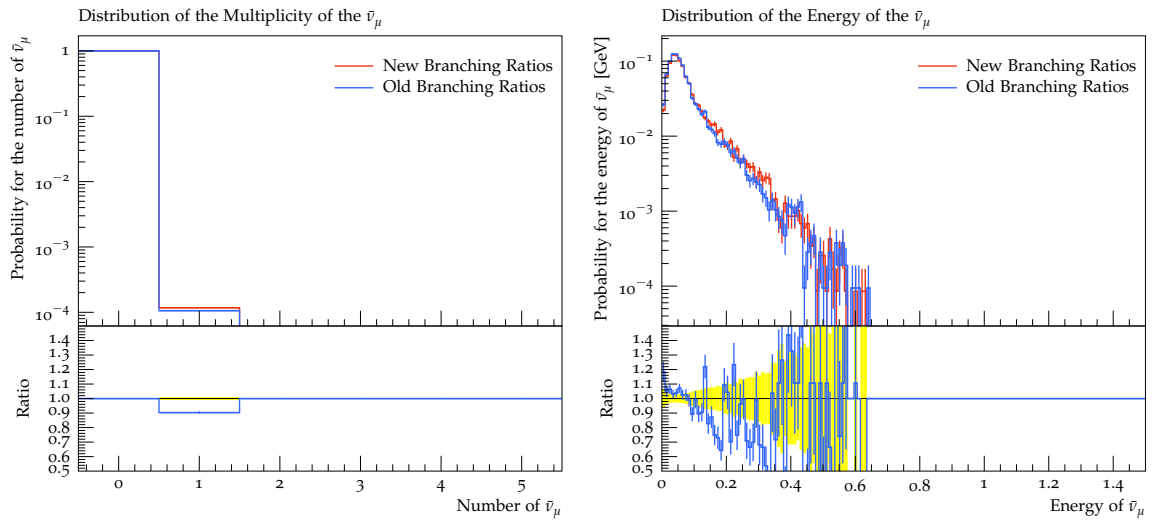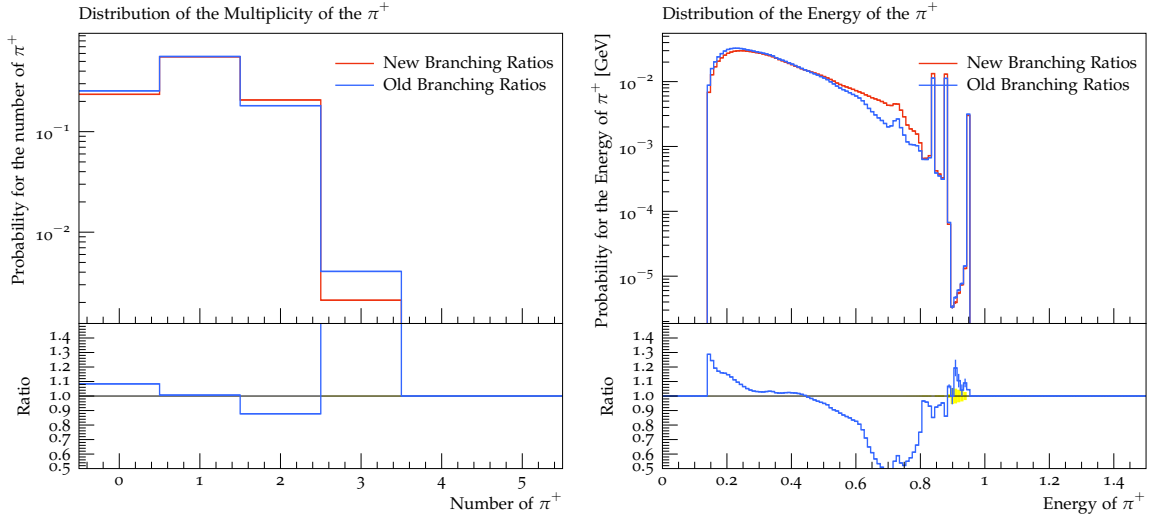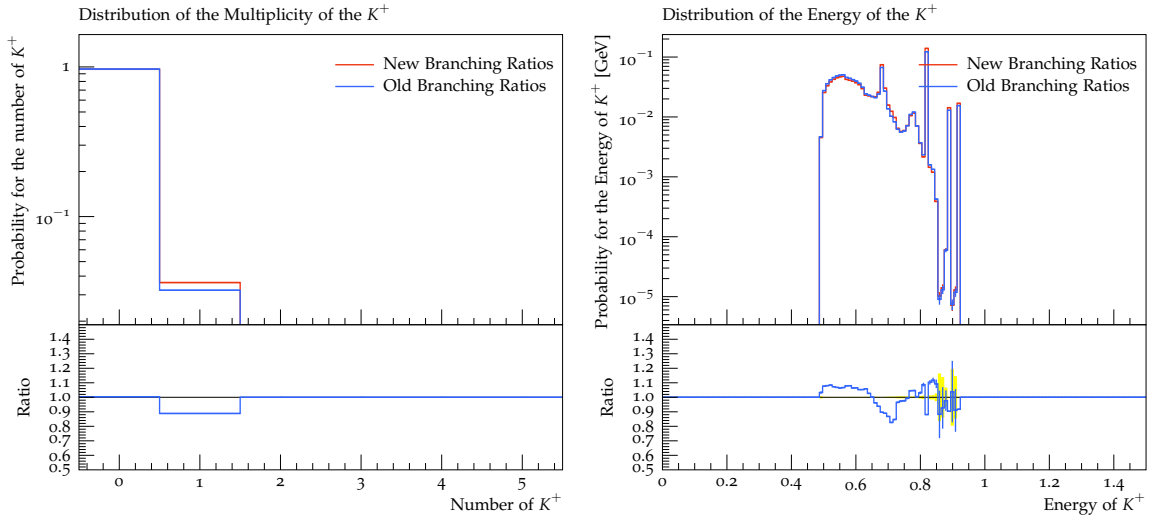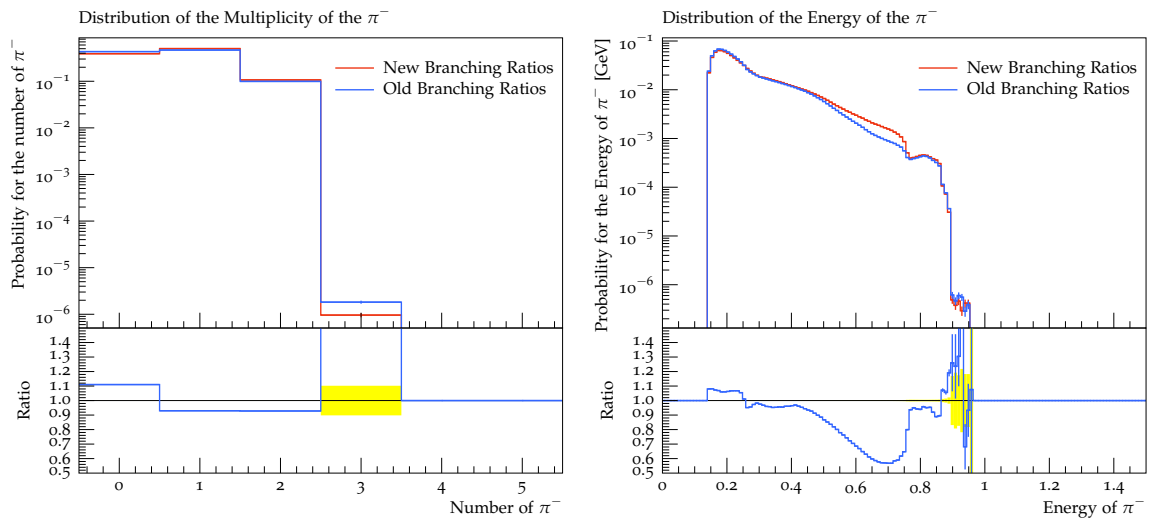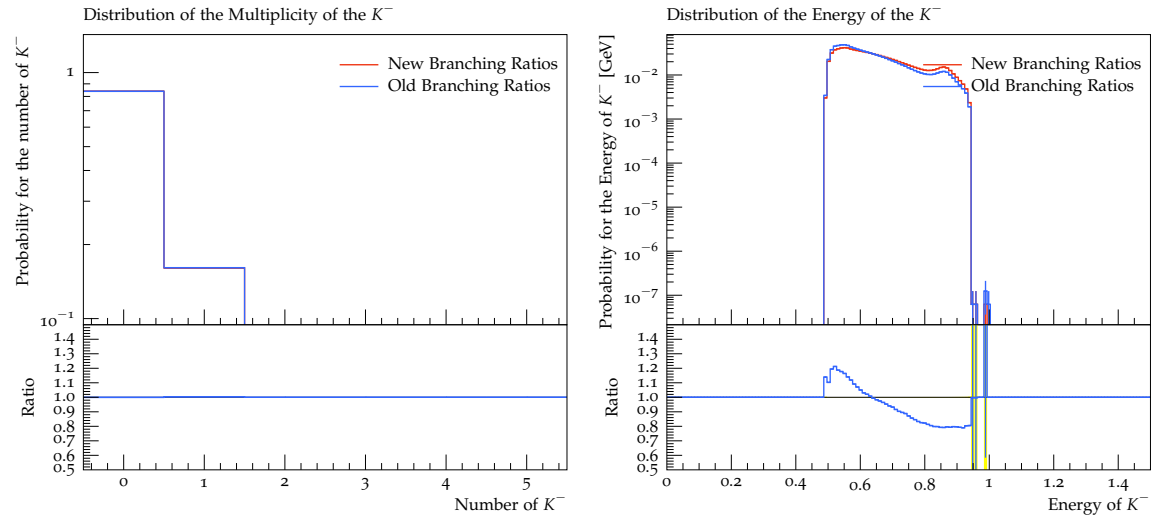
Figure A.6: multiplicity and energy spectrum of the π
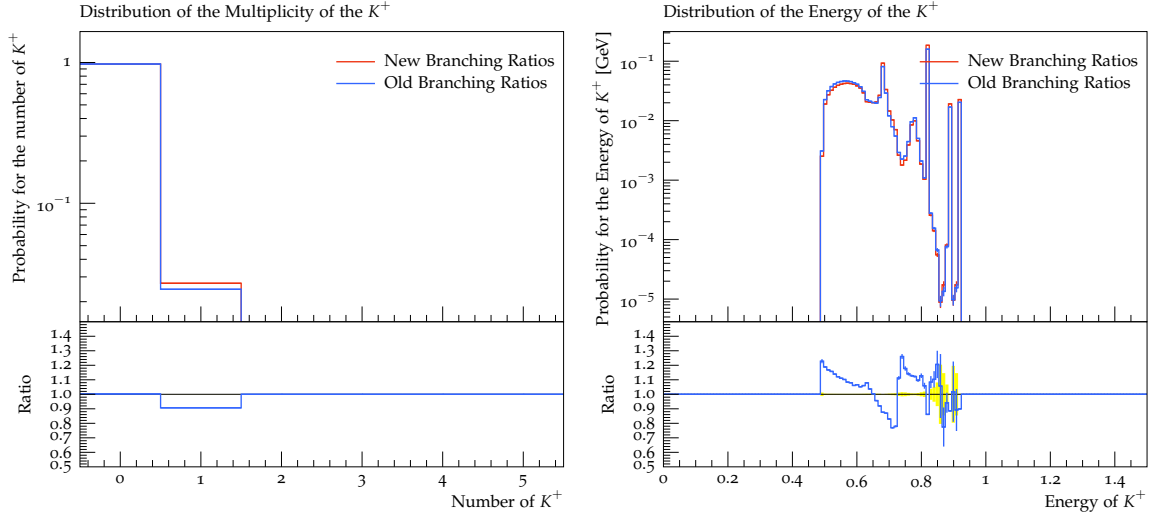
Figure A.7: multiplicity and energy spectrum of the K^+
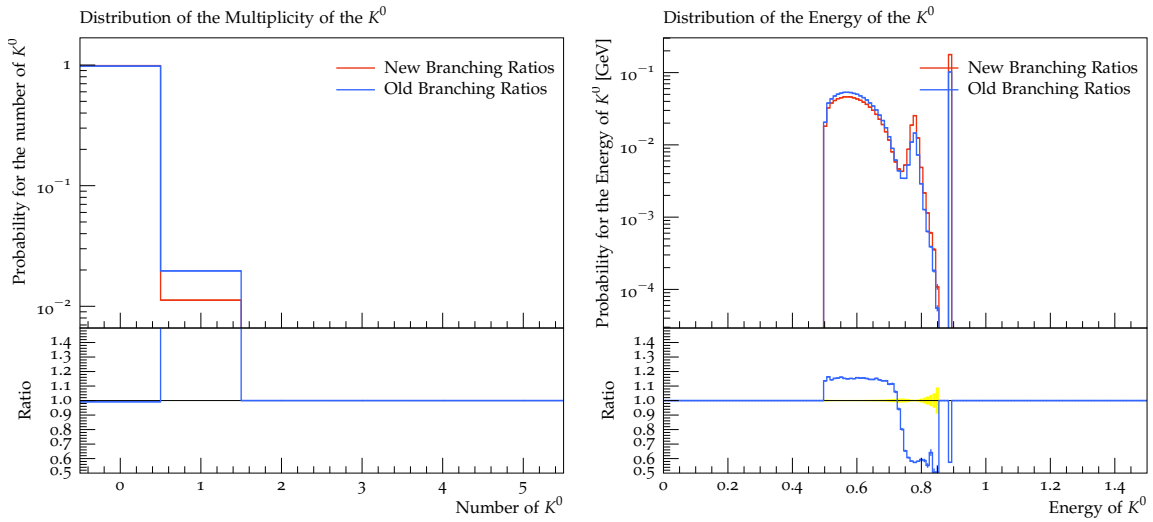
Figure A.8: multiplicity and energy spectrum of the K
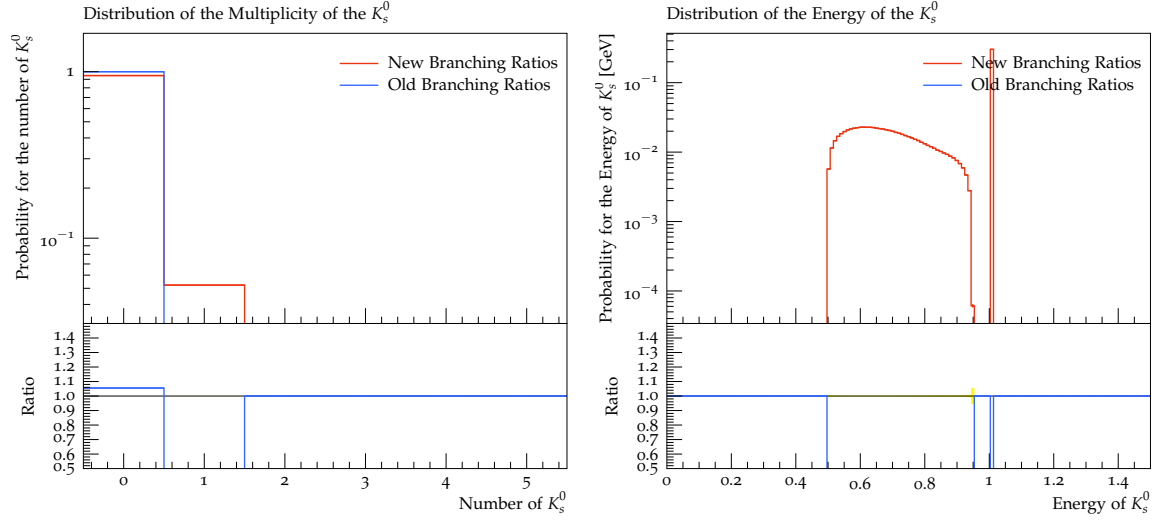
Figure A.9: multiplicity and energy spectrum of the K_s
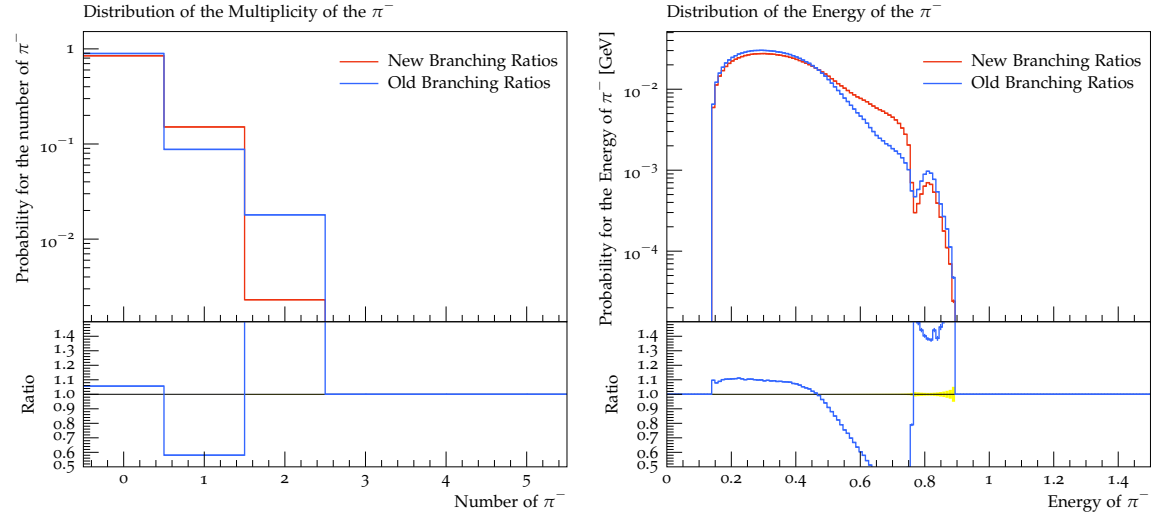
Figure A.10: multiplicity and energy spectrum of the π^-
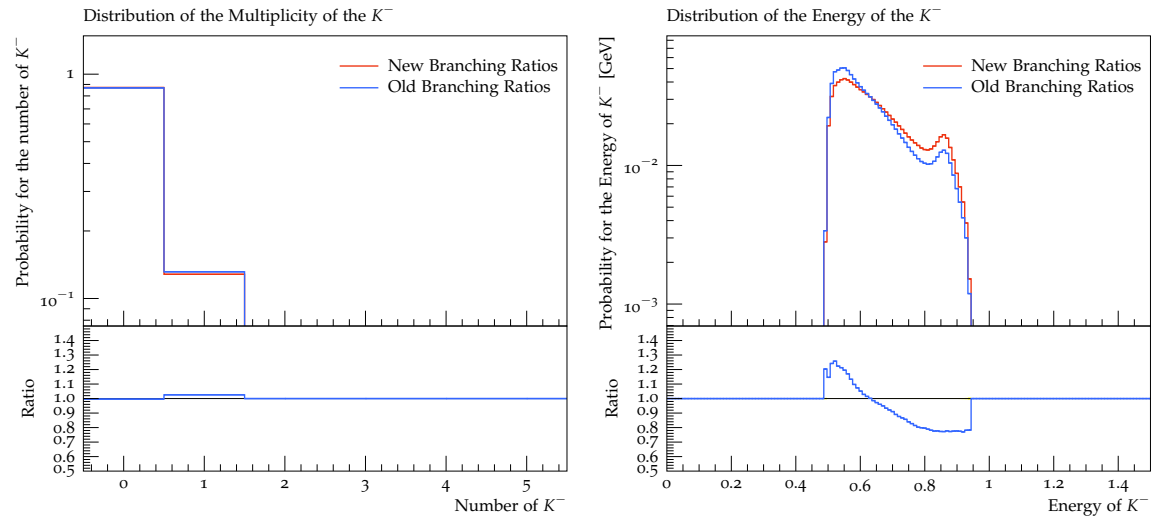
Figure A.11: multiplicity and energy spectrum of the K^-
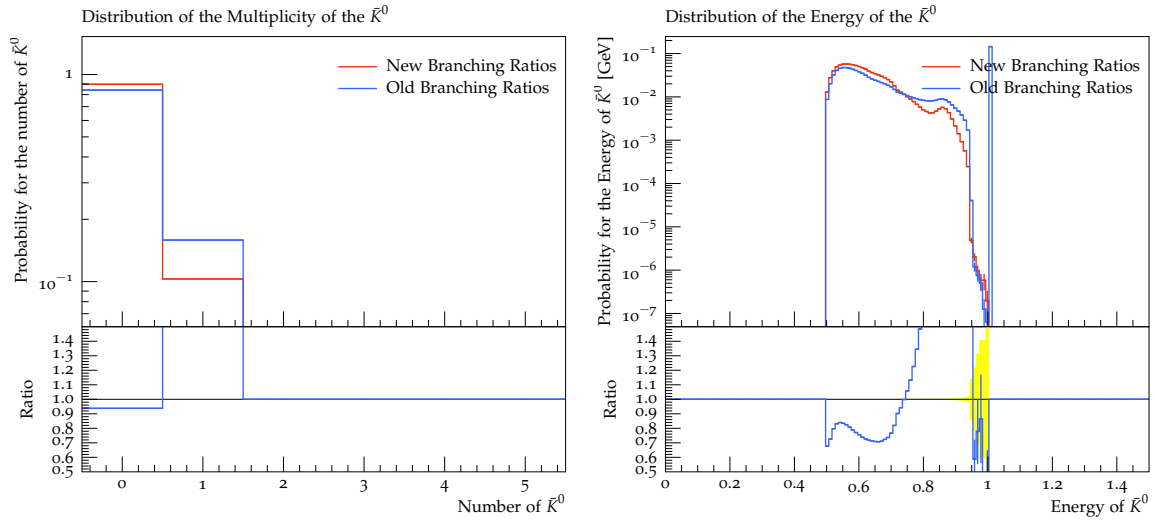
Figure A.12: multiplicity and energy spectrum of the $\bar{K}$

A.3 Complete Decays
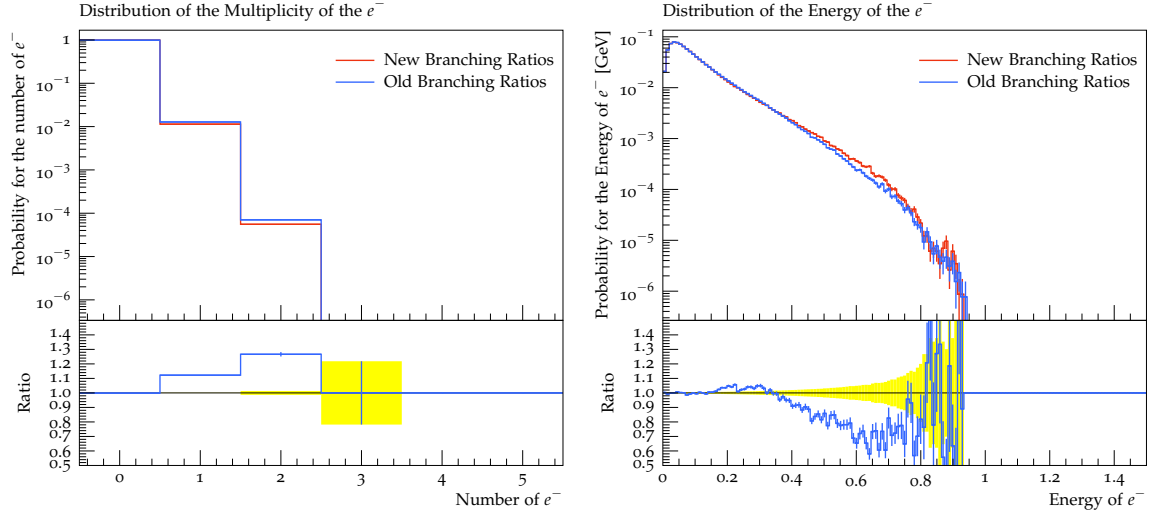
Figure A.13: multiplicity and energy spectrum of the e^-
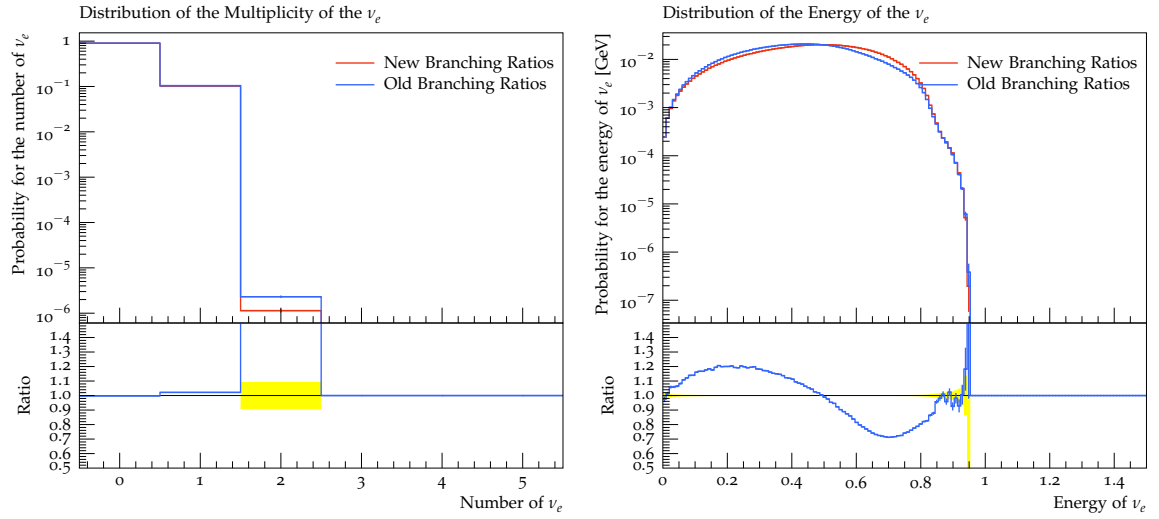
Figure A.14: multiplicity and energy spectrum of the ν_e^-

Figure A.15: multiplicity and energy spectrum of the μ^-

Figure A.16: multiplicity and energy spectrum of the ν_μ^-

Figure A.17: multiplicity and energy spectrum of the e^+

Figure A.18: multiplicity and energy spectrum of the $\bar{\nu}_e$

Figure A.19: multiplicity and energy spectrum of the μ^+

Figure A.20: multiplicity and energy spectrum of the $\bar{\nu}_\mu$

Figure A.21: multiplicity and energy spectrum of the π^+

Figure A.22: multiplicity and energy spectrum of the K^+

Figure A.23: multiplicity and energy spectrum of the π^-

Figure A.24: multiplicity and energy spectrum of the K^-

A.4 Form Factor Models

A.4.1 $\Lambda_c^+ \to \Lambda + l^+ + \nu_l$
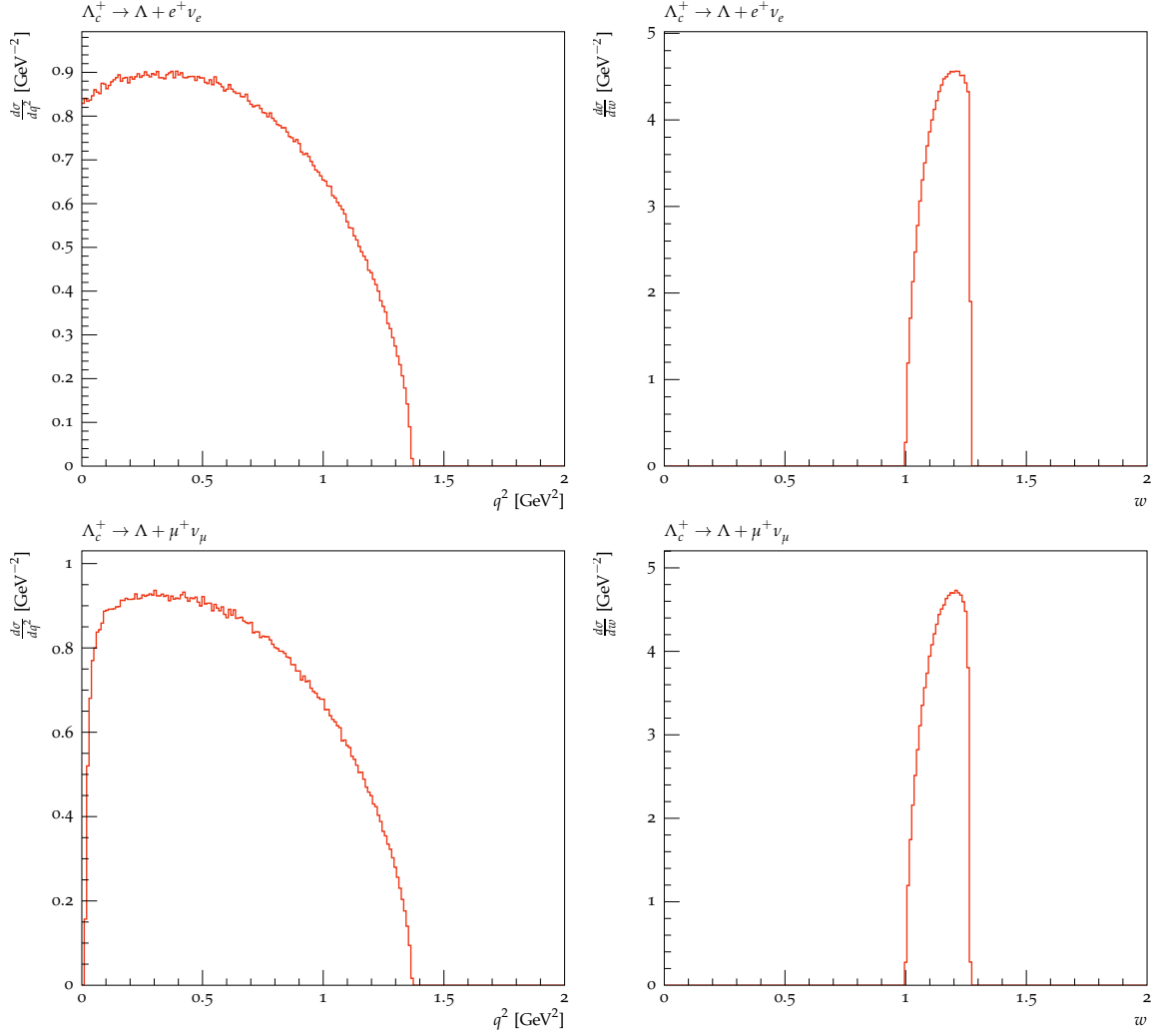
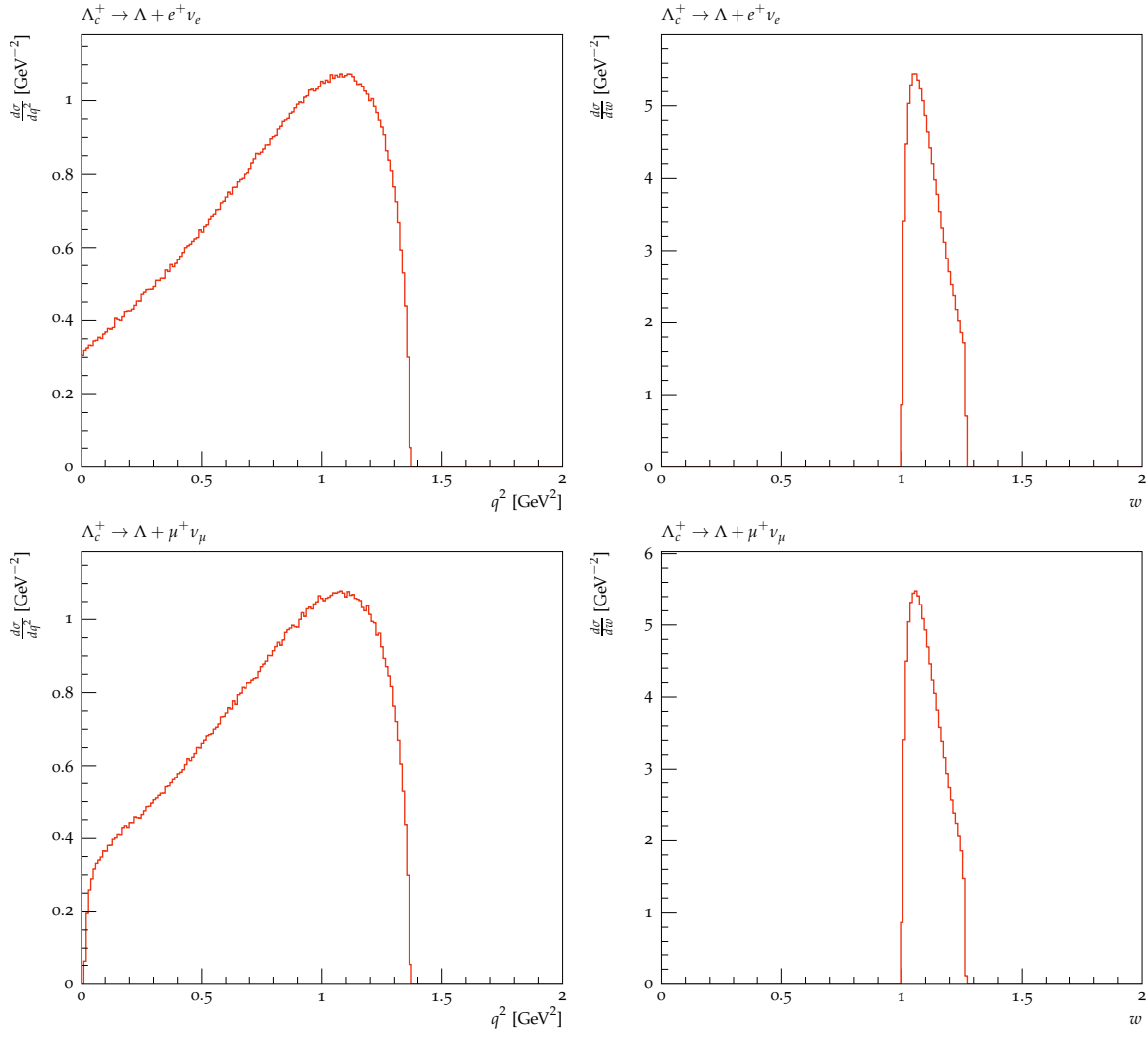**Figure A.25:** q^2 and w in the semileptonic decay into e (up) and μ (down) with the Λ in the CCQM

A.4.2 $\Lambda_c^+ \to n + l^+ + \nu_l$
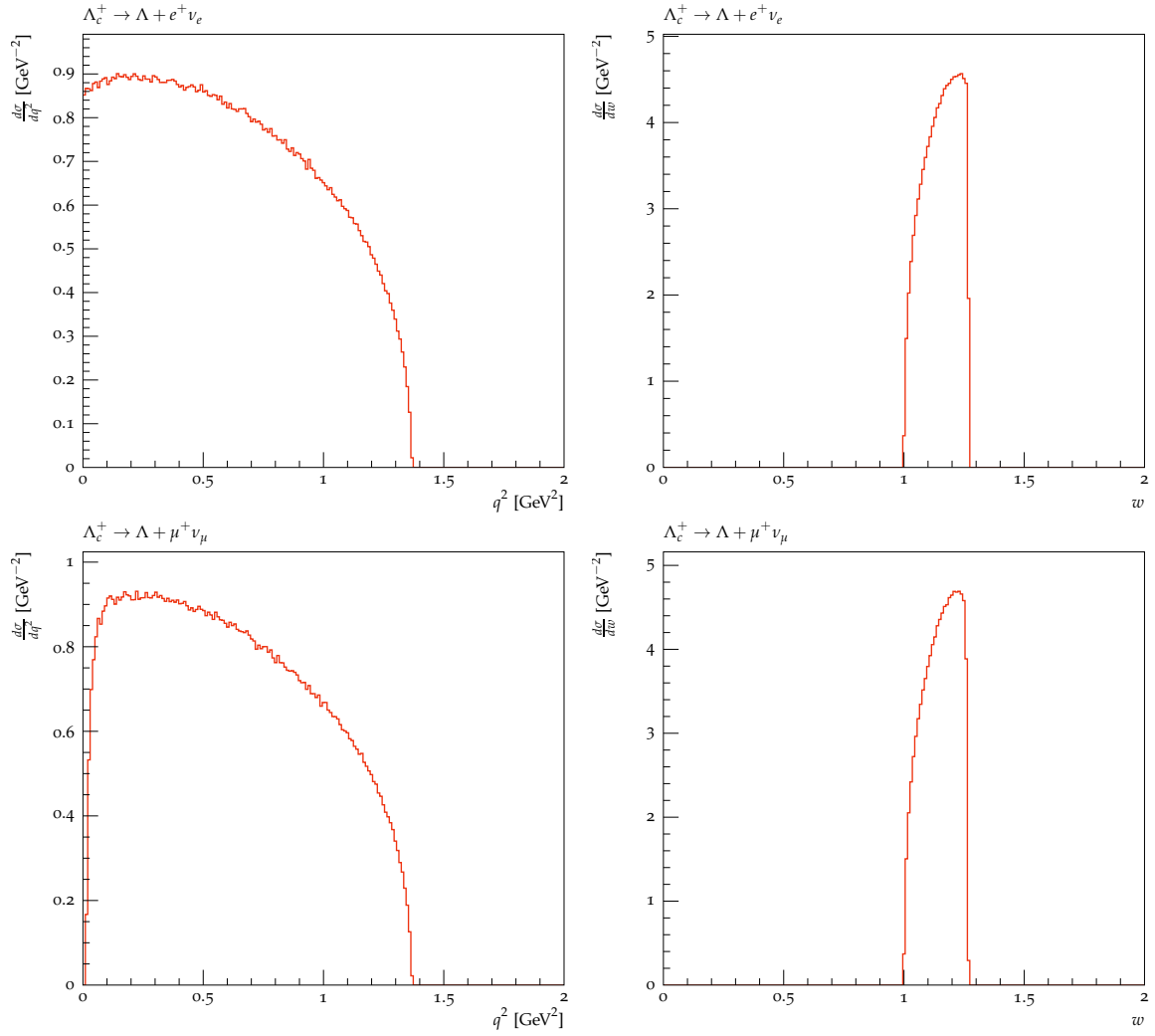
Figure A.26: q^2 and w in the semileptonic decay into e (up) and μ (down) with the Λ in the RQM
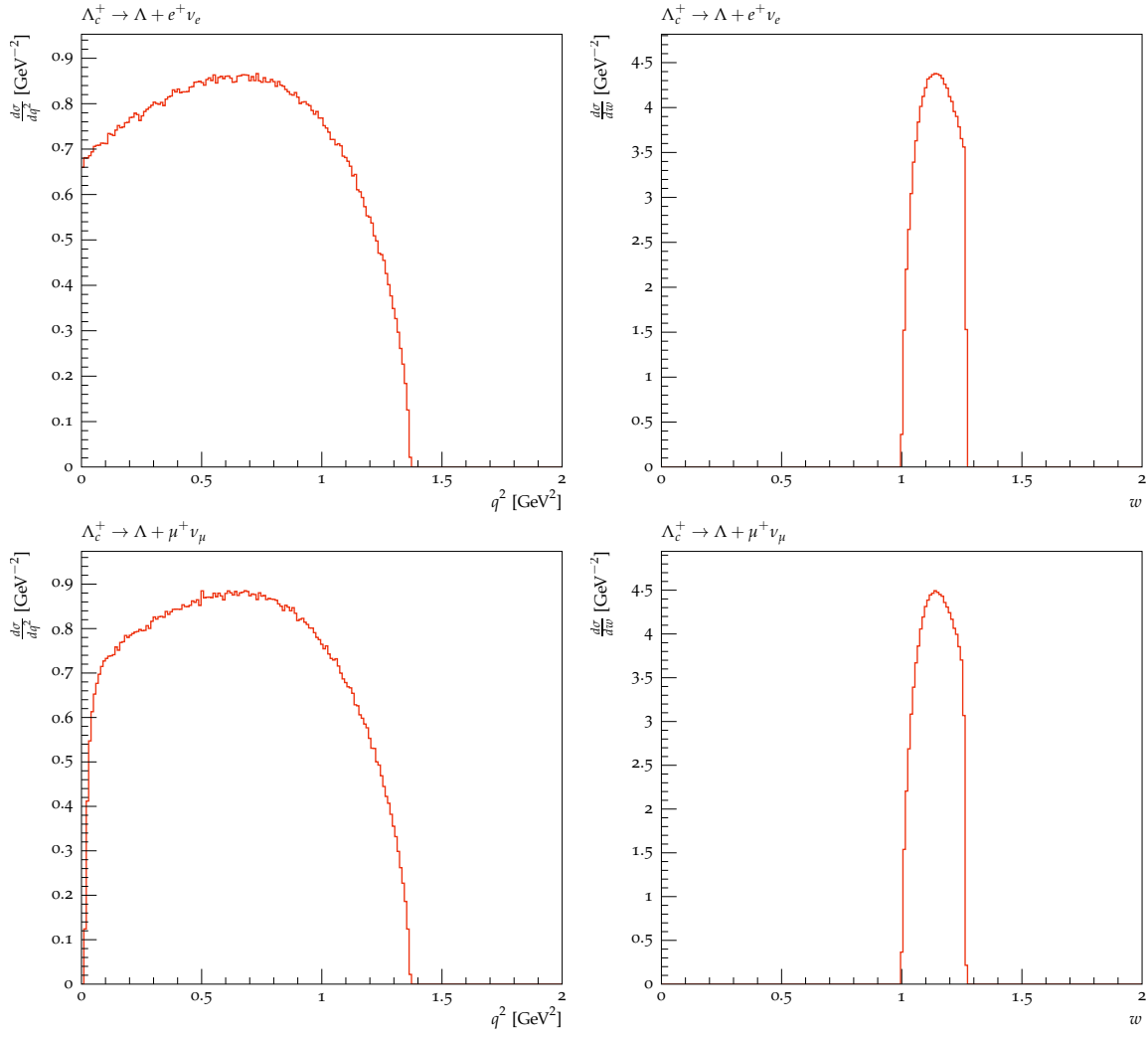
Figure A.27: q^2 and w in the semileptonic decay into e (up) and μ (down) with the Λ in the LCSR Twist 3
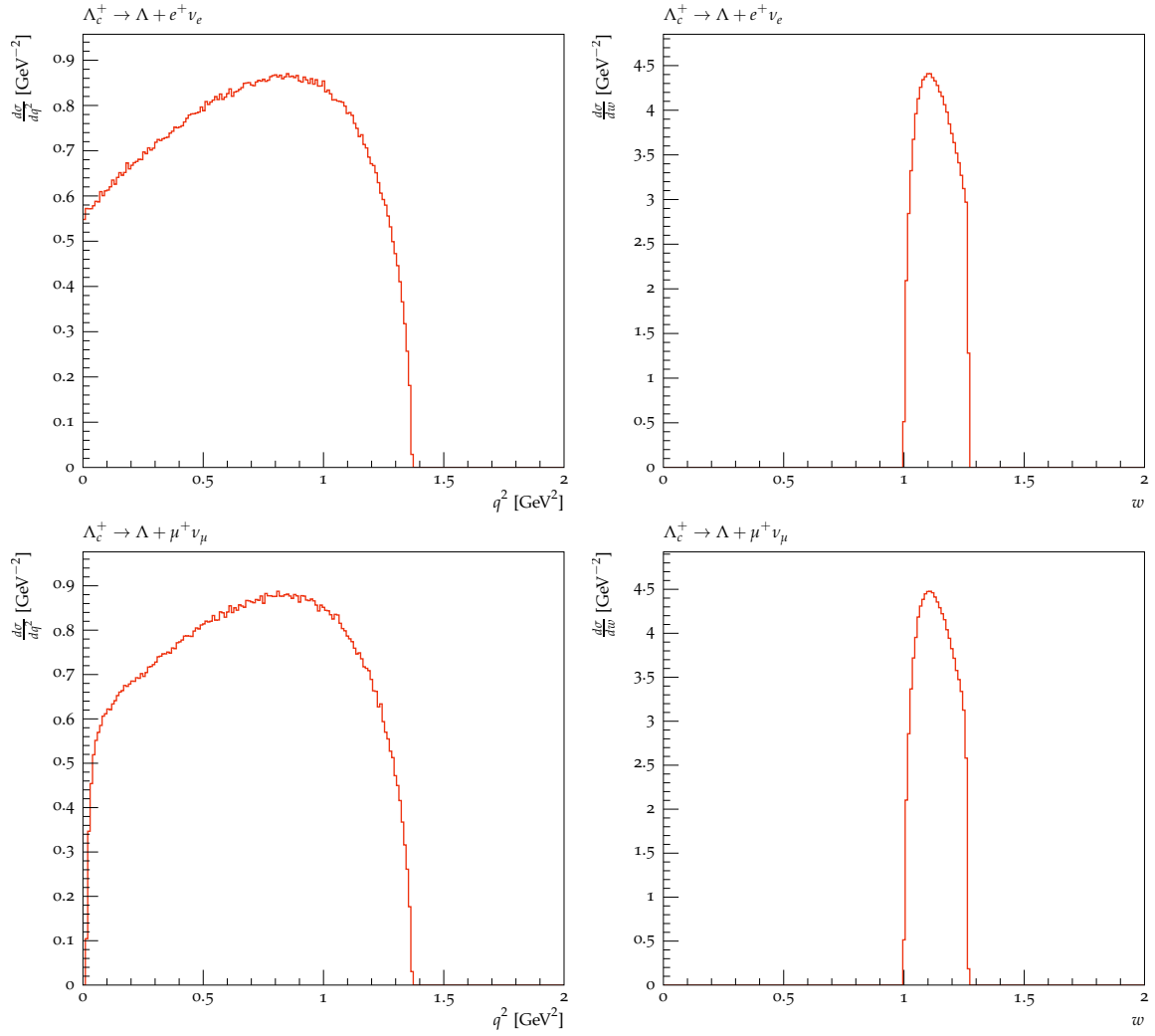
Figure A.28: q^2 and w in the semileptonic decay into e (up) and μ (down) with the Λ in the LCSR twist 6
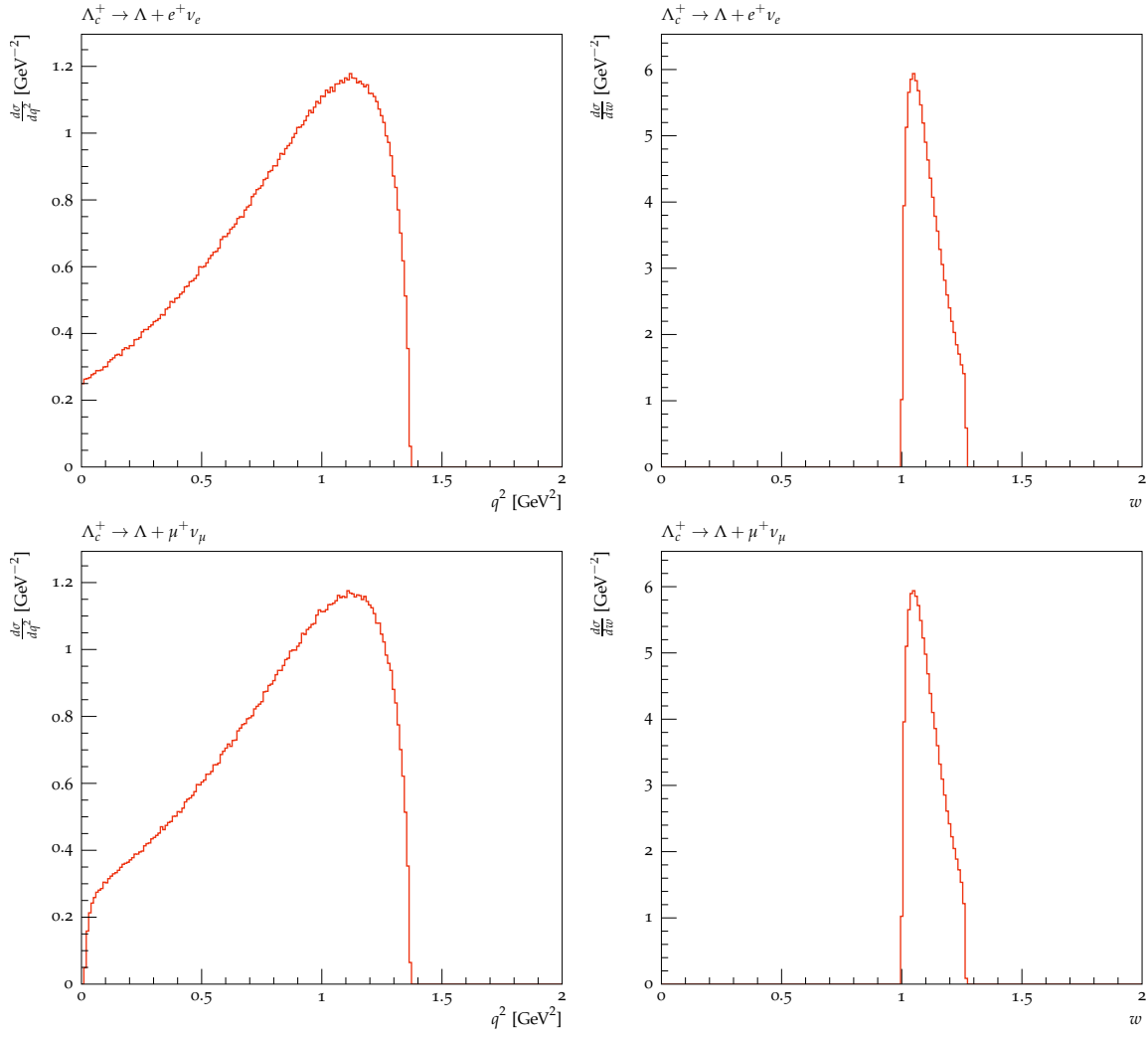
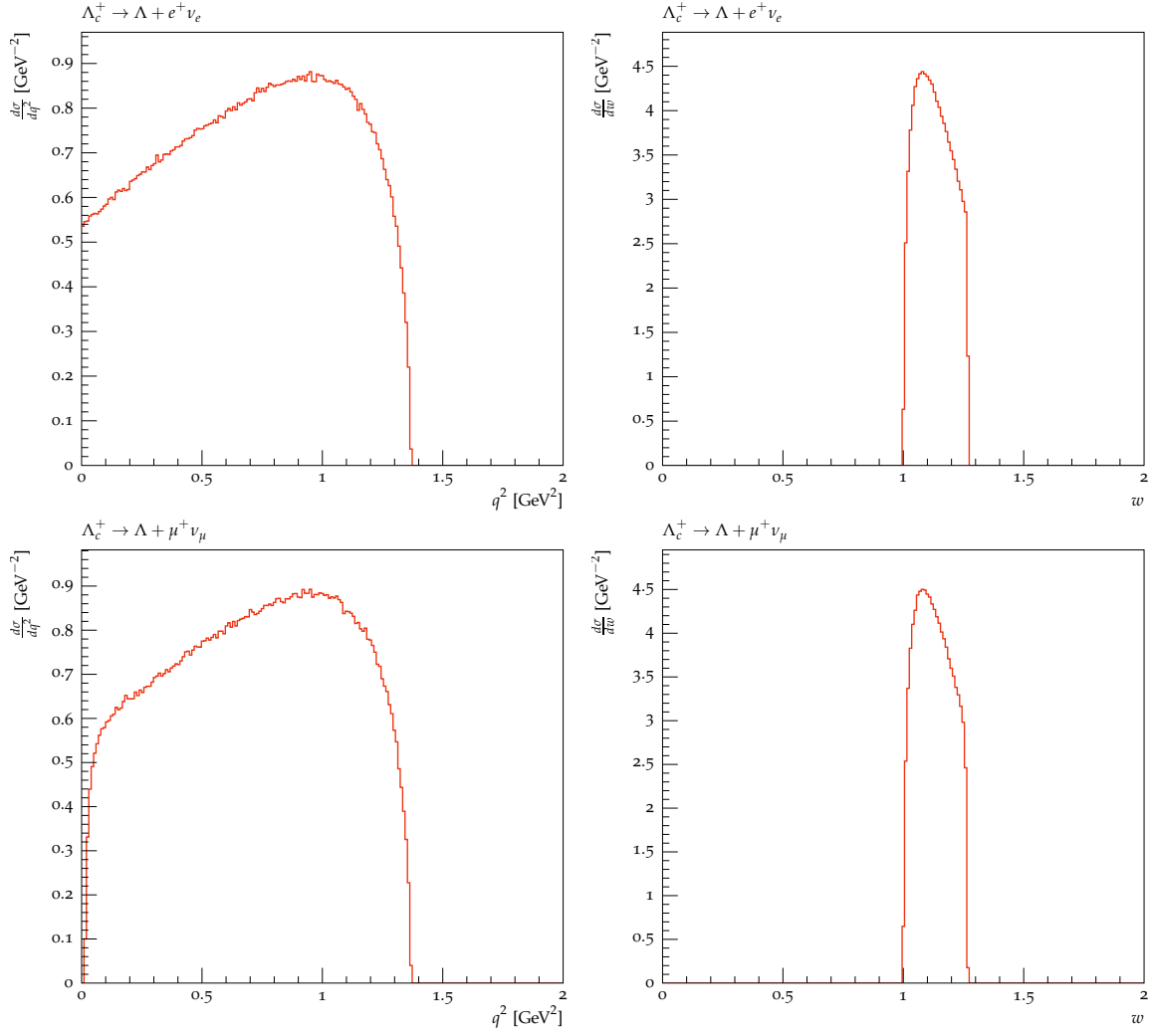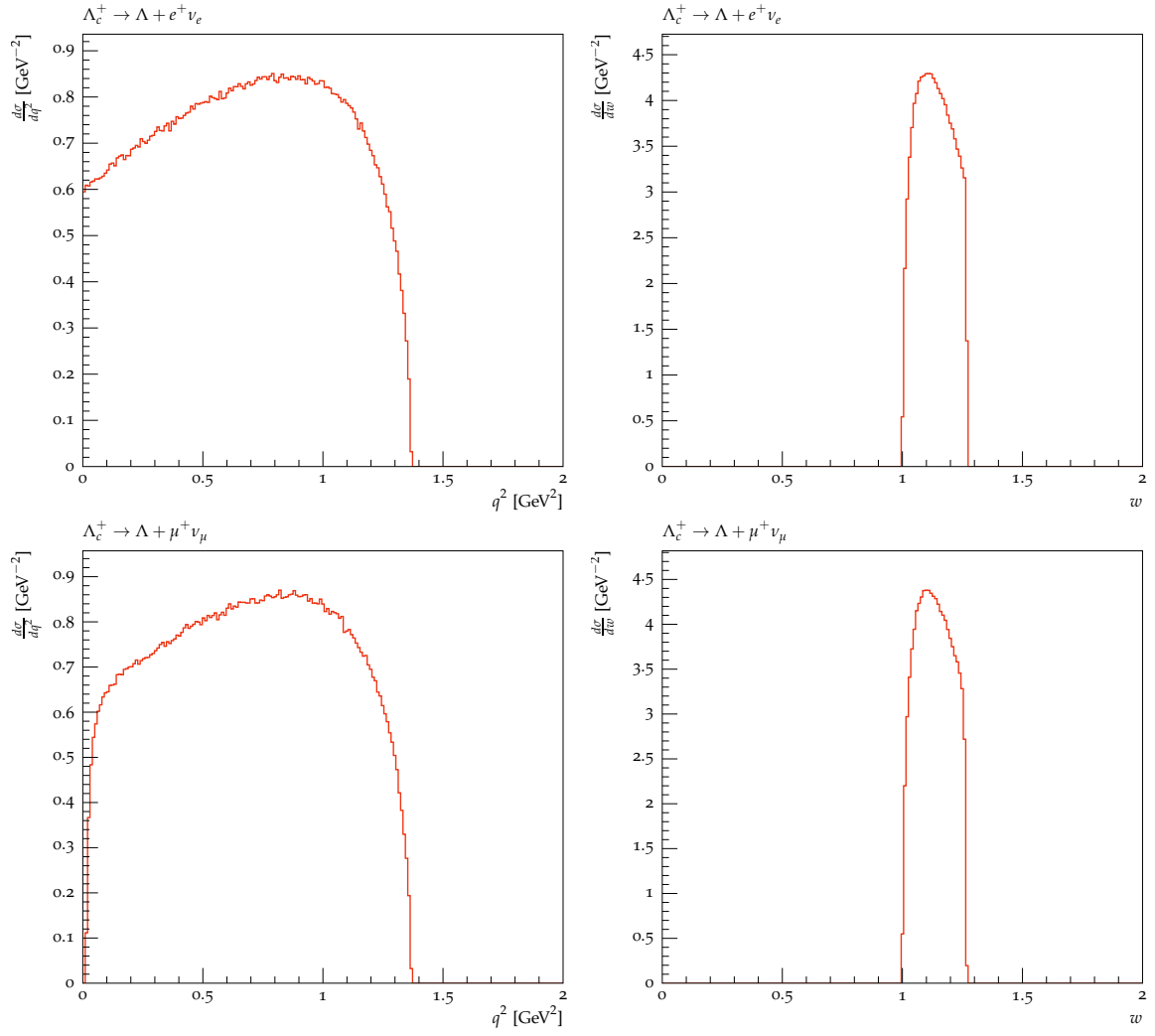**Figure A.29:** q^2 and w in the semileptonic decay into e (up) and μ (down) with the Λ in the QCDSR Full | Rectangular | 1
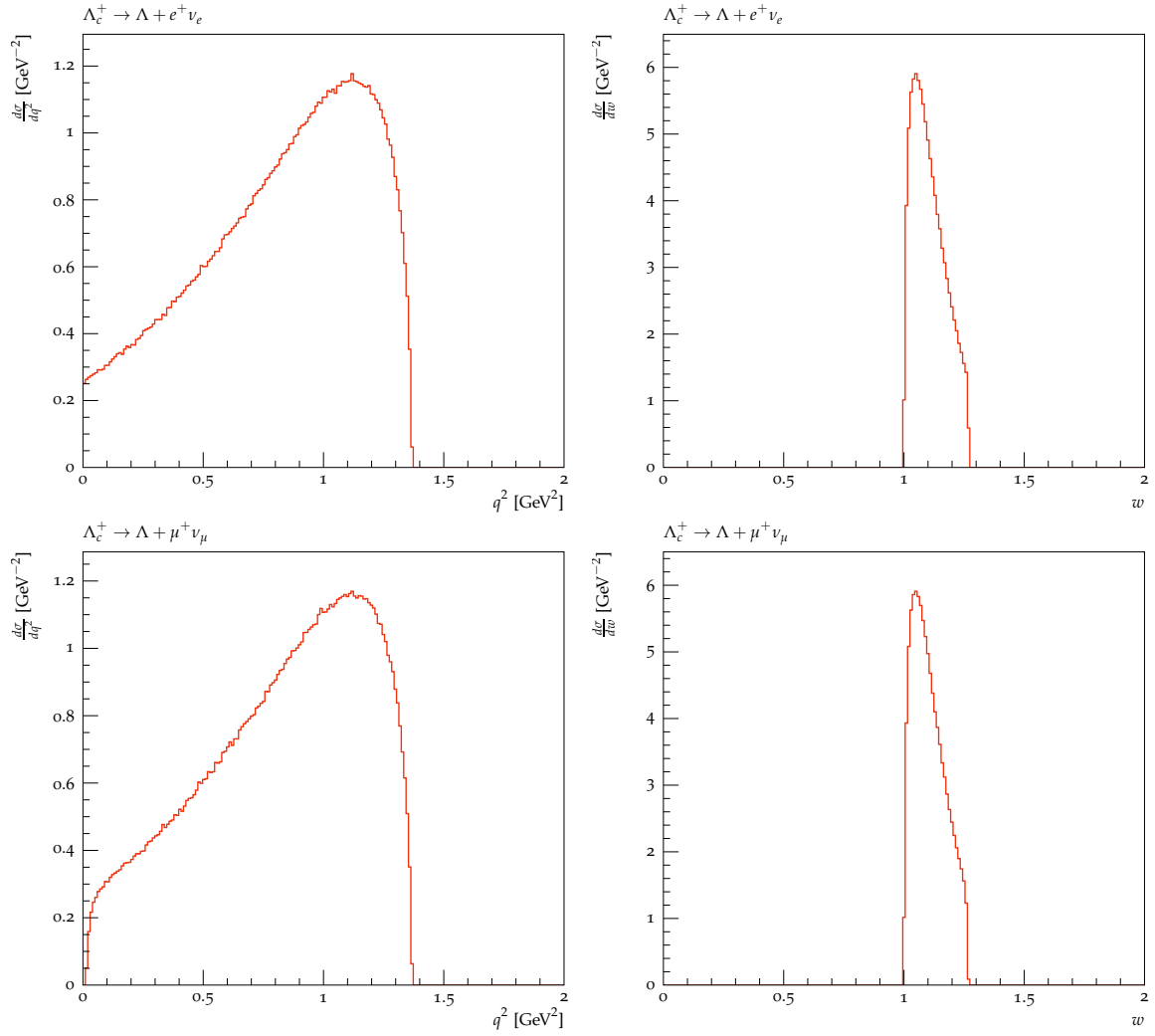
Figure A.30: q^2 and w in the semileptonic decay into e (up) and μ (down) with the Λ in the QCDSR Full | Rectangular | 2

Figure A.31: q^2 and w in the semileptonic decay into e (up) and μ (down) with the Λ in the QCDSR Full | Triangular | 1
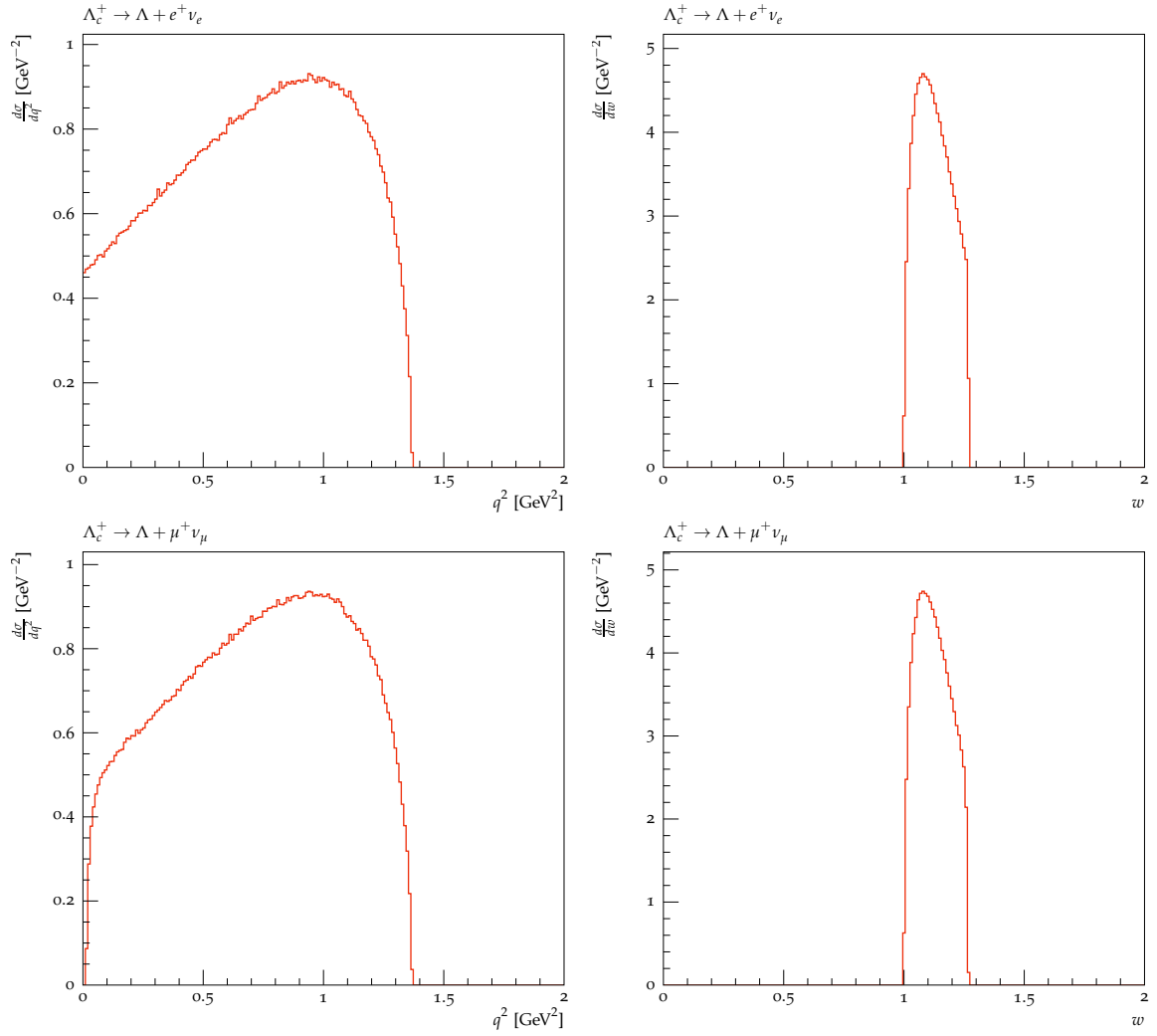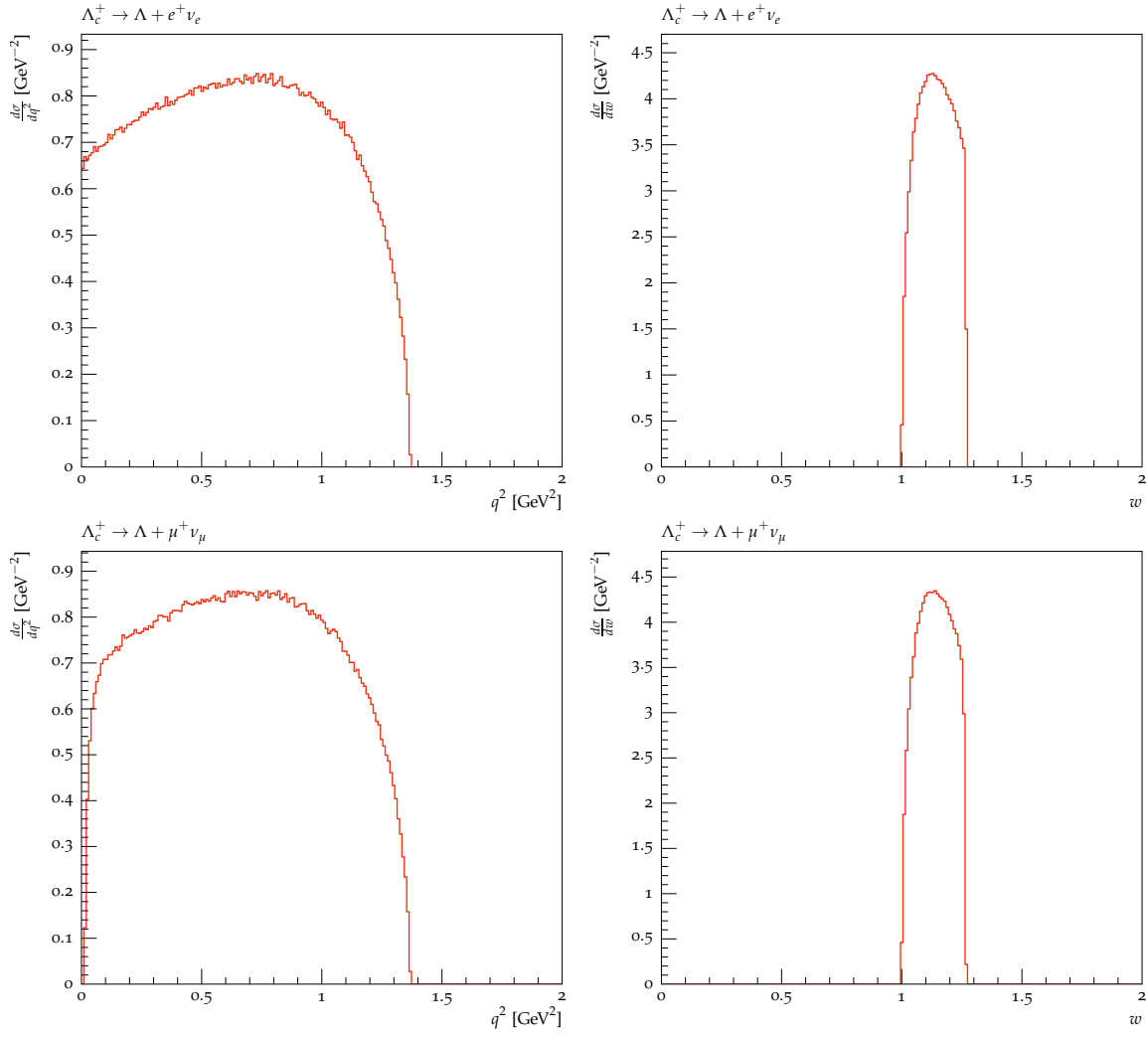
Figure A.32: q^2 and w in the semileptonic decay into e (up) and μ (down) with the Λ in the QCDSR Full | Triangular | 2
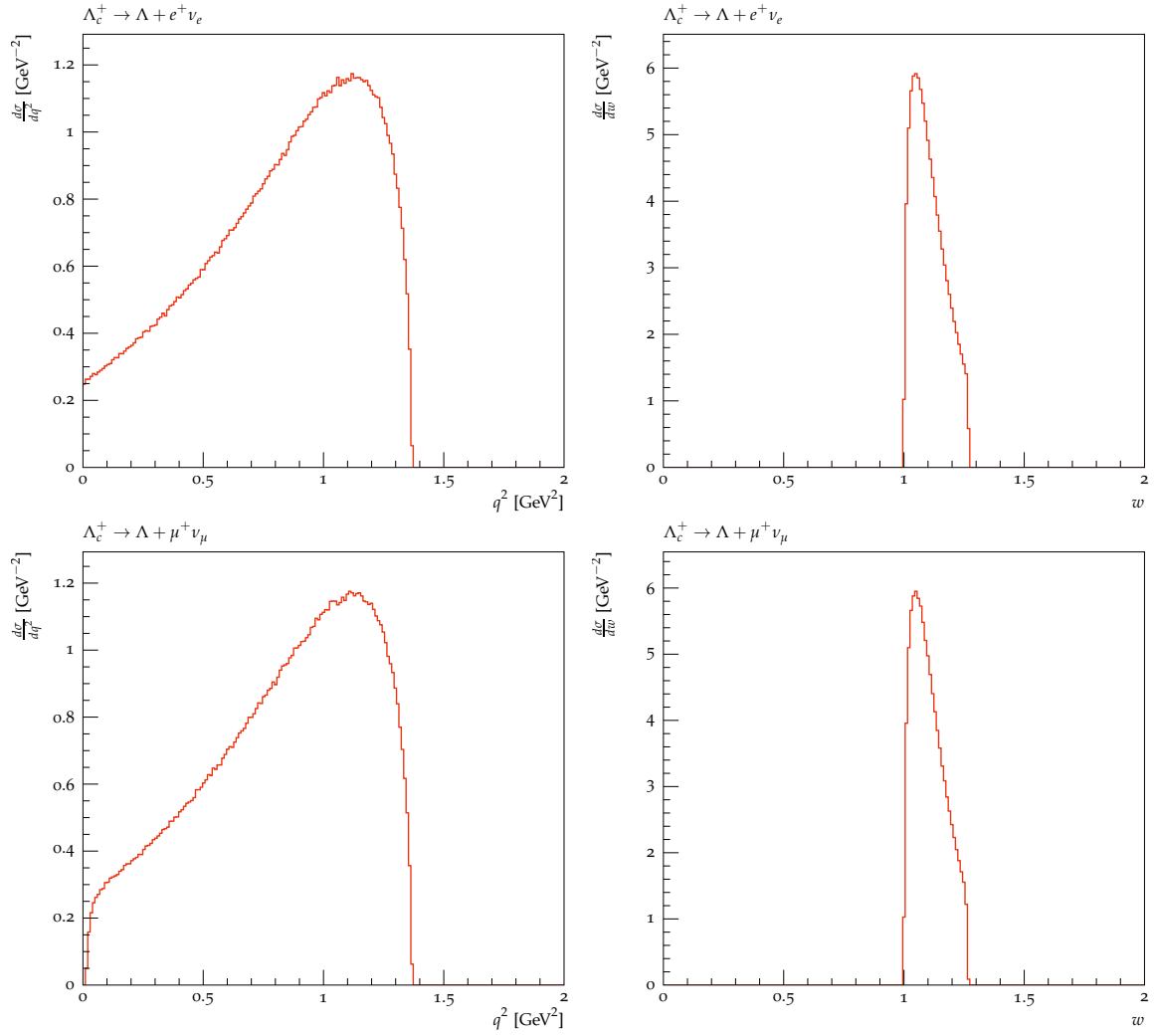
Figure A.33: q^2 and w in the semileptonic decay into e (up) and μ (down) with the Λ in the QCDSR Pole | Rectangular | 1
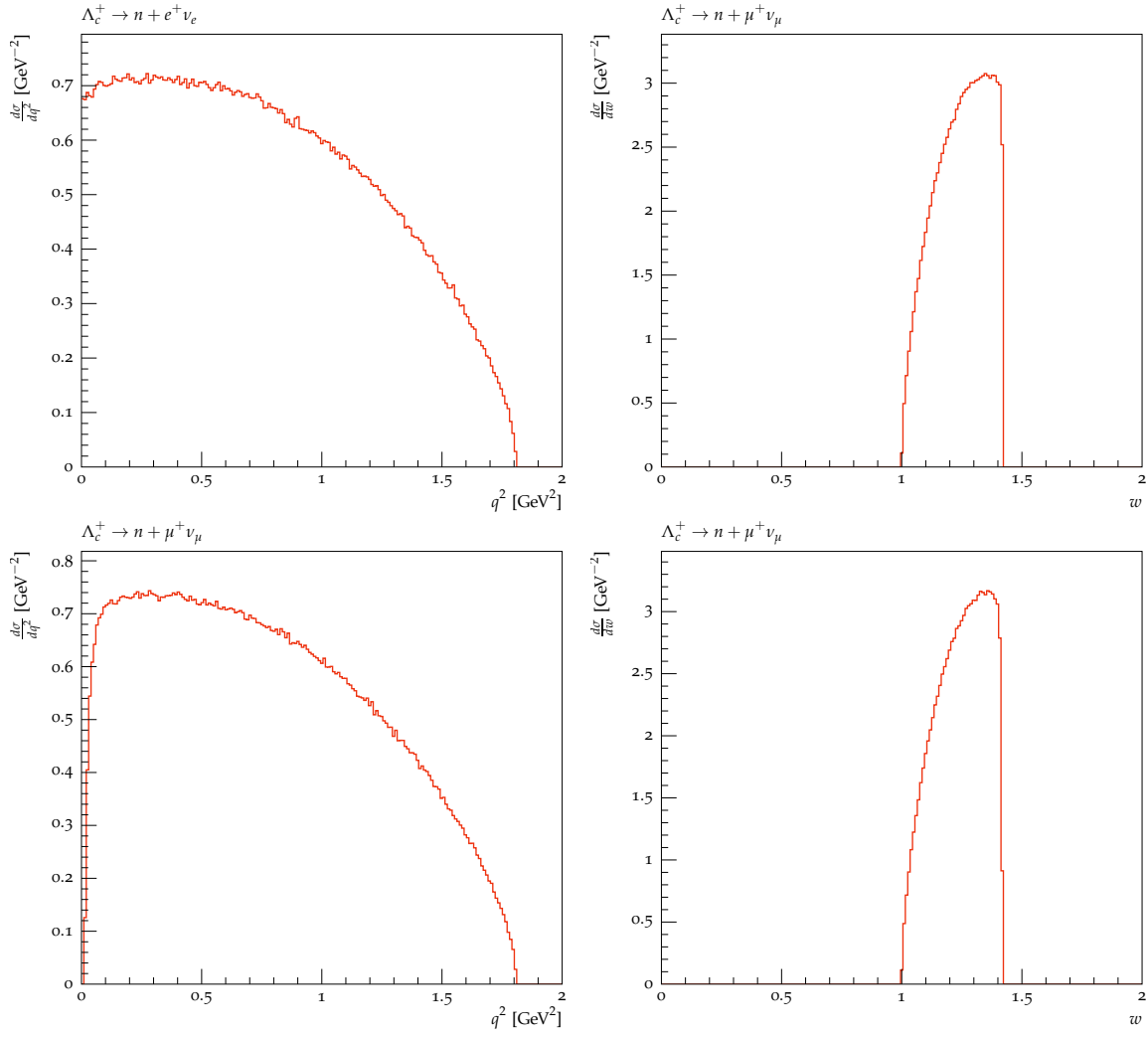
Figure A.34: q^2 and w in the semileptonic decay into e (up) and μ (down) with the Λ in the QCDSR Pole | Rectangular | 2

Figure A.35: q^2 and w in the semileptonic decay into e (up) and μ (down) with the Λ in the QCDSR Pole | Triangular | 1
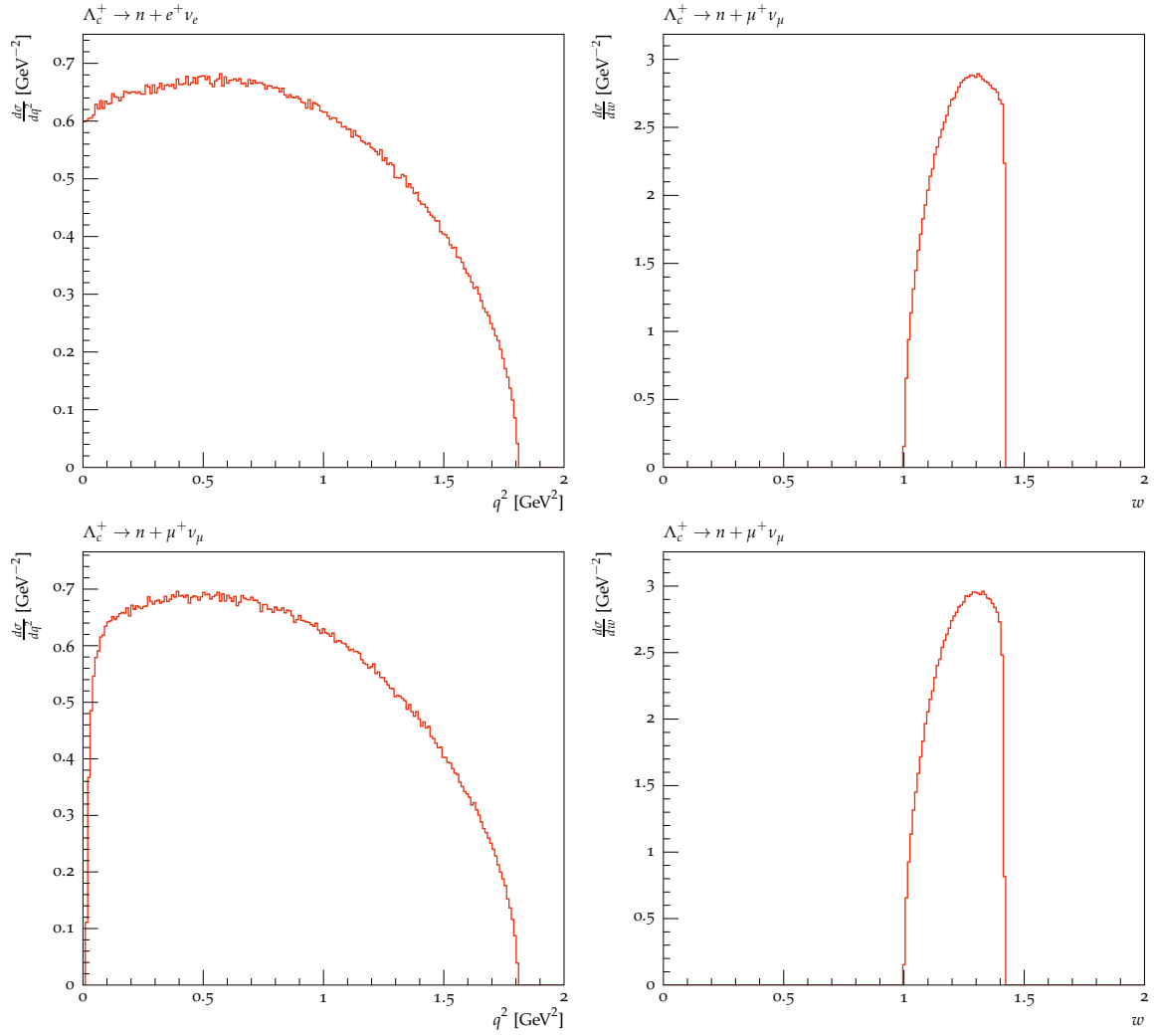
Figure A.36: q^2 and w in the semileptonic decay into e (up) and μ (down) with the Λ in the QCDSR Pole | Triangular | 2

Figure A.37: q^2 and w in the semileptonic decay into e (up) and μ (down) with the neutron in the CCQM

Figure A.38: q^2 and w in the semileptonic decay into e (up) and μ (down) with the neutron in the RQM

Erklärung

Hiermit erkläre ich, dass ich diese Arbeit im Rahmen der Betreuung am Institut für Kern- und Teilchenphysik ohne unzulässige Hilfe Dritter verfasst und alle Quellen als solche gekennzeichnet habe.

Sven Schiffner
Dresden, Mai 2017